FOILING SuMoth CHALLENGE

RAFALE

ÉTS Le génie pour l'industrie

ÉCOLE DE TECHNOLOGIE SUPÉRIEURE

Université du Québec

Foiling SuMoth Challenge Stage 1 - 2024

DESIGN, MANUFACTURING & SUSTAINABILITY

Sponsored by

11TH HOUR RACING

MARINESHIFT360

PERSICO

Bcomp®

RAFALE ETS | ETS, MONTREAL, CANADA | rafale@etsmtl.ca

ABSTRACT

This document presents the work done by RAFALE ETS to produce a sustainable Moth sailing dinghy. This prototype called Rafale IV has been produced during the 2023-2024 season by a team of 21 students. Most of the boat has been built during the past year, but some parts are reused and modified from the last prototype (rig, wings and parts of the wand). Firstly, the design process is explained for each new part, including hypothesis, calculations, and results. Secondly, the theoretical manufacturing approach is presented. It involves the material use, the processes, and the forecast SuMoth budget balance. Finally, a life cycle analysis of the project is presented, with comments about the sustainable approach of the team for building the boat.

Table of contents

LIST OF TABLES 6
LIST OF FIGURES 7
INTRODUCTION 9
1 ENGINEERING AND DESIGN 10
1.1 Technical specifications 10
1.2 Hull Design 10
1.2.1 Load cases study 10
1.2.2 Safety factor 12
1.2.3 Material selection 12
1.2.4 Material mechanical testing 14
1.2.5 External and internal design 16
1.2.6 Structural design with FEM 18
1.3 Gantry 19
1.4 Hydrofoil system 20
1.4.1 Design requirements analysis 20
1.4.2 Optimization programs 22
1.4.3 Hydrofoil design 27
1.4.4 Hydrofoil FEM validation 28
1.4.5 Validation of the hydrofoil system through CFD analysis 29
1.5 Wand 30
1.5.1 Design requirements analysis 30
1.5.2 Optimization programs 30
1.5.3 Design 30
1.5.4 FEA 31
1.6 Wings 32
1.7 Rig 32
1.7.1 Mast step 32
1.7.2 Vang Lever 33
1.7.3 Spreader 34
1.7.4 Deck fittings 35
1.8 Electronics and data acquisition 35
1.9 Performance prediction with a DVPP 36
2 MANUFACTURING AND COST ANALYSIS 38

2.1 General description 38
2.2 Hull 39
2.2.1 Hull molds 39
2.2.2 Infusion, assembly and finish 40
2.3 Gantry 41
2.4 Hydrofoil system 41
2.4.1 Daggerboard shaft and rudder shaft 41
2.4.2 Metal additive manufacturing 41
2.4.3 Hydrofoils wings manufacturing 42
2.5 Wand 42
2.6 Wings 42
2.7 Rig 43
2.7.1 Mast step 43
2.7.2 Spreader 43
2.7.3 Vang lever 43
2.8 Onboard electronic system 43
2.9 Materials 44
2.9.1 Elium thermoplastic resin 44
2.9.2 Flax / Elium composite 44
2.9.3 Carbon / Elium composite 44
2.9.4 3D printed recycled PET 44
2.9.5 PET foam core 44
2.10 Cost analysis 45
3 SUSTAINABILITY ANALYSIS 47
3.1 General description 47
3.2 Boat and elements lifecycle 47
3.2.1 Design and Rafale III 47
3.2.2 Molds 47
3.2.3 Composites 47
3.2.4 Processes and energies 48
3.2.5 Scraps, Expired and Reused Materials 48
3.3 End-of-Life Plan 48
3.4 Theorical LCA 49
3.5 Actions for a sustainable future 49
4 TEAM 50

4.1 Team members 50
4.2 Sponsors 50
5 MARINESHIFT 360 LCA 51
5.1 General description 51
5.1.1 Functional unit 51
5.1.2 Outline 51
5.1.3 Assumptions 51
5.2 Boat and elements lifecycle 52
5.2.1 Hull 52
5.2.2 Gantry 52
5.2.3 Hydrofoils 53
5.2.4 Wings 53
5.2.5 Wand 53
5.2.6 Rigging 54
5.2.7 Consumables 55
5.2.8 Hardware 55
5.2.9 Processes 56
5.2.10 Transport of the boat 56
5.3 Results and analysis 56
5.3.1 Impact categories 56
5.3.2 Team transportation 60
5.3.3 Rafale III & IV comparison 62
5.4 Conclusion 64
6 BIBLIOGRAPHY 65
A. APPENDIX A 66

LIST OF TABLES

Table 1.1 External and internal force balances for critical navigation 11
Table 1.2 Failure modes of flax / Elium® tensile specimens 14
Table 1.3 Results of mechanical tests on flax / Elium® composite 15
Table 1.4 Summary of the requirements for the performance part 21
Table 1.5 Summary of mechanical strength requirements 22
Table 1.6 Values of optimization results for the daggerboard wing 23
Table 1.7 Values of optimization results for the rudder wing 24
Table 1.8 CFD results for the daggerboard wing 25
Table 1.9 CFD results for the two wings 25
Table 2.1 Cost analysis of Rafale IV 45
Table 5.1 Hull modeling on MS360 52
Table 5.2 Gantry modeling on MS360 52
Table 5.3 Hydrofoils modeling on MS360 53
Table 5.4 Wings modeling on MS360 53
Table 5.5 Wand modeling on MS360 53
Table 5.6 Vand modeling on MS360 54
Table 5.7 Spreader modeling on MS360 54
Table 5.8 Mat step modeling on MS360 54
Table 5.9 Fittings modeling on MS360 55
Table 5.10 Consumables modeling on MS360 55
Table 5.11 Hardware modeling on MS360 55
Table 5.12 Processes modeling on MS360 56
Table 5.13 Transport of the boat modeling on MS360 56
Table 5.14 Team transport modeling on MS360 60

LIST OF FIGURES

Figure 1.1 Schematic representation of the forces applied to the Moth during navigation ((a) starboard view, (b) top view, (c) front view) 10
Figure 1.2 Internal loads 11
Figure 1.3 3D plot of dry fiber performance indexes 13
Figure 1.4 3D plot of resins performance indexes 13
Figure 1.5 Wired strain gauge (left)/ Specimen set (right) 14
Figure 1.6 Hull shape of Rafale IV 16
Figure 1.7 Deck and hull of Rafale IV 16
Figure 1.8 Main loading areas of the moth hull 17
Figure 1.9 Internal structure 17
Figure 1.10 Cross-section of hull structure mesh and detail of mesh around mast step 18
Figure 1.11 General shape of the gantry 19
Figure 1.12 : Extreme loading cases: “Nosedive” on the left and “Capsize” on the right 21
Figure 1.13 : Main dimension of the daggerboard wing 22
Figure 1.14 : Main dimension of the rudder wing 23
Figure 1.15 : Fluid domain 24
Figure 1.16 : Optimization results of the shaft, carbon laminate (right image) and basalt laminate (left image) 26
Figure 1.17 : Sketch of the proposed solutions for the wing-flap connection 27
Figure 1.18 : CAD of the hydrofoil system of Rafale IV 28
Figure 1.19 : Visualization of CFD results (takeoff on the left and flight on the right) 29
Figure 1.20 - Wand angle [°] as a function of flap angle [°] (left), flight height [mm] as a function of flap angle [°] (center), wand angle [°] and flight height [mm] as a function of foil wing angle [°] (rigth) 30
Figure 1.21 - Front section of R4 deck 30
Figure 1.22 – Outside (right) and inside (left) tube of the wand 31
Figure 1.23 - Complete R4 wand system 31
Figure 1.24 – Results of FEA on the bowsprit 32
Figure 1.25 New fittings (left), fittings molds (right) 32
Figure 1.26 Mast step CAD 33
Figure 1.27 Schematic representation of the forces applied to the lever (left) and lever CAD (right) 33
Figure 1.28 Metal inserts 34
Figure 1.29 CAD for analysis (left), CAD for manufacturing (right) 34
Figure 1.30 Spreader CAD 35
Figure 1.31 Deck fittings 35
Figure 1.33 Example of polar plot 37

Figure 1.34 Influence of the boat's CG position on the area used by the skipper 38
Figure 2.1 CEAD AM Flexbot robot and its environment 39
Figure 2.2 Hull mold CAD 40
Figure 2.3: CAD drawing of the print bed 42
Figure 3.1 Comparison of the impact of carbon (orange), flax (green) and basalt (blue) fibers on climate change 48
Figure 5.1 Scope and Boundaries of the LCA on MS360 51
Figure 5.2 Rafale IV's impact on global warming (fossil) 57
Figure 5.3 Rafale IV's impact on global warming (non fossil) 57
Figure 5.4 Rafale IV's impact on mineral resource scarcity 58
Figure 5.5 Rafale IV's impact on energy consumption (non-renewable) 58
Figure 5.6 Rafale IV's impact on energy consumption (renewable) 59
Figure 5.7 Rafale IV's impact on water consumption 59
Figure 5.8 Rafale IV's impact on marine eutrophication 60
Figure 5.9 Impact of team transportation on the climate change category 61
Figure 5.10 Impact of team transportation on the mineral resource scarcity category 61
Figure 5.11 Impact of team transportation on the energy consumption (non-renewable) category 62
Figure 5.12 Comparison of the impact of Rafale IV and III on climate change (fossil) 62
Figure 5.13 Comparison of the impact of Rafale IV and III on climate change (non fossil) 63
Figure 5.14 Comparison of the impact of Rafale IV and III on mineral resource scarcity 63
Figure 5.15 Comparison of the impact of Rafale IV and III on marine eutrophication 64

INTRODUCTION

The season 2023-3024 has been busy at Rafale ETS. During the last 10 month, our 21 team members worked hard to design and produce a new prototype. There have even been two master's theses written about this project; one on the hull and the other on the hydrofoils. We really improved our manufacturing methods since the last concept, but also welcomed new sponsors and had the opportunity to present our work at a boat show.

Our team would like to thank all our sponsors for supporting us! The knowledge, materials, products, services, and money that has been integral to the design and to the production of the newest prototype. We would also like to thank ETS for offering us an incredible workspace and access to state-of-the-art equipment and tools. Finally, we would like to thank the SuMoth organization and team for giving us the opportunity to participate in such an enriching competition, pushing us and our project into an invigorating, innovative, and sustainable direction.

This document first details the design methods and calculations for the new parts of the boat. Then, it presents the theoretical manufacturing approaches and the associated SuMoth budget balance. Finally, our vision of sustainability and our related practices are explained based on a LCA made with MS360.

The entire team is proud to present their new SuMoth concept: Rafale IV !

1 ENGINEERING AND DESIGN

1.1 Technical specifications

Based on the club's past experience and objectives for the season, a functional specification for the Rafale IV sailboat has been drawn up. The latter can be consulted in APPENDIX A.

1.2 Hull Design

1.2.1 Load cases study

To dimension the Rafale IV sailing dinghy hull, the cases of stable flight in strong wind conditions (20 knots) and righting are taken into consideration. Critical cases such as nosediving are considered by a dynamic safety factor. The safety factor used for the design will be presented below.

When sailing on the foils, the Moth is subjected to various external forces that can be divided into three categories:

- Gravitational forces and buoyancy
- Aerodynamic forces
- Hydrodynamic forces

They are, overall, like those applied on a conventional sailboat. But, since the Moth flies on T-shaped foils, hydrodynamic drag and lift forces are added to these appendages. These forces are shown schematically in Figure 1.1. It's also important to consider the boat's internal forces. These are mainly associated with the pre-tensioning of the rig via the forestay, shrouds, and vang, which generate compression in the mast. These forces are far from negligible since they can be of the order of a ton. Figure 1.2 shows them from the hull's point of view.

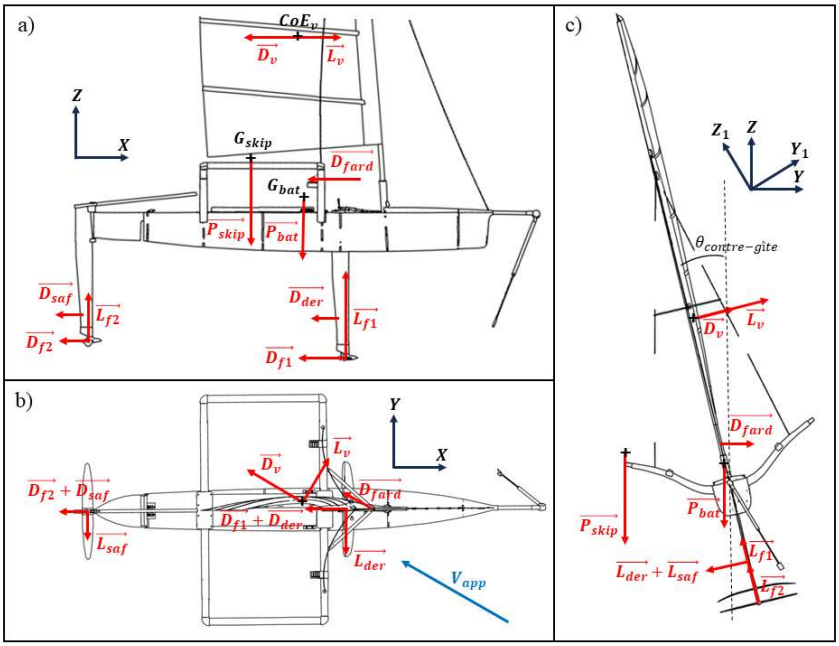

Figure 1.1 Schematic representation of the forces applied to the Moth during navigation ((a) starboard view, (b) top view, (c) front view)

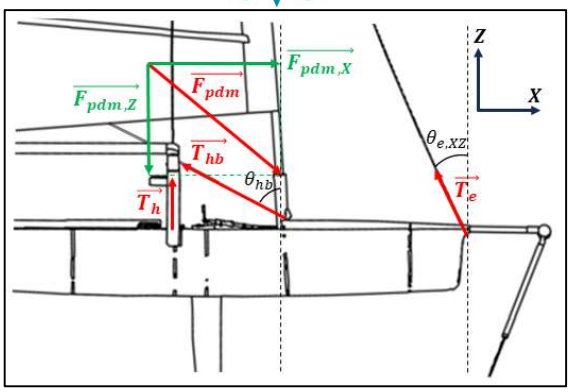

Figure 1.2 Internal loads

The forestay is tensioned using a system of 4:1 pulleys to pre-tension the rig. Then, the vang is tensioned (48:1 pulley system) and loads the forestay. It is assumed that tensioning the boom vang does not relieve the shrouds, so they remain pre-tensioned.

To estimate the forces in the critical flight case, whose values will be used for the dimensioning, we base ourselves on the results obtained with the following conditions:

- Maximum wind at 20 knots
- Skipper mass =80 kg
- Counter-heel = 40°
- 90%/10% weight distribution on daggerboard foil and rudder foil respectively

A static and a dynamic approach have been used for calculations. The results are shown in the Table 1.1. The construction of the DVPP will be developed in a specific section. It can estimate a greater number of forces than static modeling. There is a difference of 43% in the results for forces in the hydrofoils. This is because the DVPP considers the entire acceleration phase of the sailboat at all true wind angles. Drag forces are neglected for the structural dimensioning of the hull.

Table 1.1 External and internal force balances for critical navigation

		DVPP [N]	Static [N]
External loads	Main foil lift	1498,3	1045,5
	Rudder foil lift	166,5	116,2
	Sail force X	869,4	
	Sail force Y	597,55	599,6
	Windage X	224,1	
	Windage Y	336,2	
	Hull drag (before takeoff)	258,8	
	Main foil drag	62,1	
	Daggerboard drag	34	
	Rudder drag	20,6	
	Rudder foil drag	12,4	
	Anti-drift force (no drift)		375,2

		DVPP [N]	Static [N]
Internal loads	Tension shroud		1369,7
	Tension forestay		4391,3
	Tension boom-vang		12000
	Force mast stump X		12377,6
	Force mast stump Z		11867,1

1.2.2 Safety factor

A safety factor of 1.2 is applied to the design. This is based on the recommendations of (Hollaway, 1994) and is broken down into several sub-factors. It is calculated using the following equation:

$$f_s = \gamma_{f1} \cdot \gamma_{f2} \cdot \gamma_{m1} \cdot \gamma_{m2} \cdot \gamma_n$$

With:

- γ_{f1}=deviation of loads from calculated values=1.05.
- γ_{f2}=load estimation errors=1.
- γ_{m1}=material property deviation=1.05.
- γ_{m2}=local weaknesses due to geometric or manufacturing defects=1.1.
- γ_n=economic or health risks of breakage=1.

1.2.3 Material selection

To choose a composite material adapted to the structural but also environmental constraints for the manufacture of the hull, preliminary research is carried out in the literature and the technical documentation of the various suppliers of resin or fiber which seem interesting to meet these requirements.

The graphs shown in Figure 1.3 and Figure 1.4 can be obtained using performance indexes based on the recommendations of (M. F. Ashby, 2011) and (Michael F. Ashby & Dupeux, 2011). They can be used to help select the dry fibers and resins best suited to the constraints of rigidity, mechanical strength, and environmental impact. Each of them groups the three performance indexes associated with each material, namely:

- Index favoring mass reduction and stiffness maximization M1= ρ/E
- Index favoring mass reduction and mechanical strength maximization M2=ρ/R_m
- Index favoring mass reduction and ecological impact M3=ρ.(GHG emissions).

The lower the value of an index, the better the material's performance in relation to it.

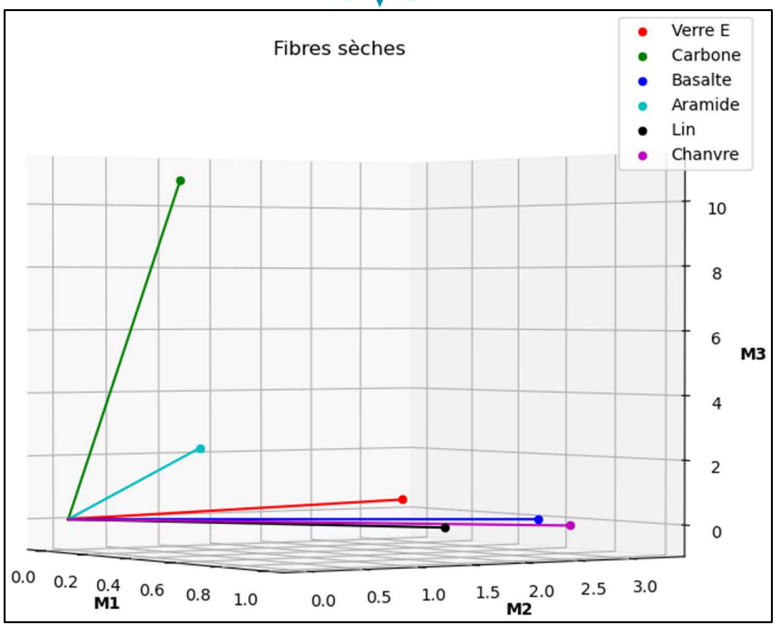

Figure 1.3 3D plot of dry fiber performance indexes

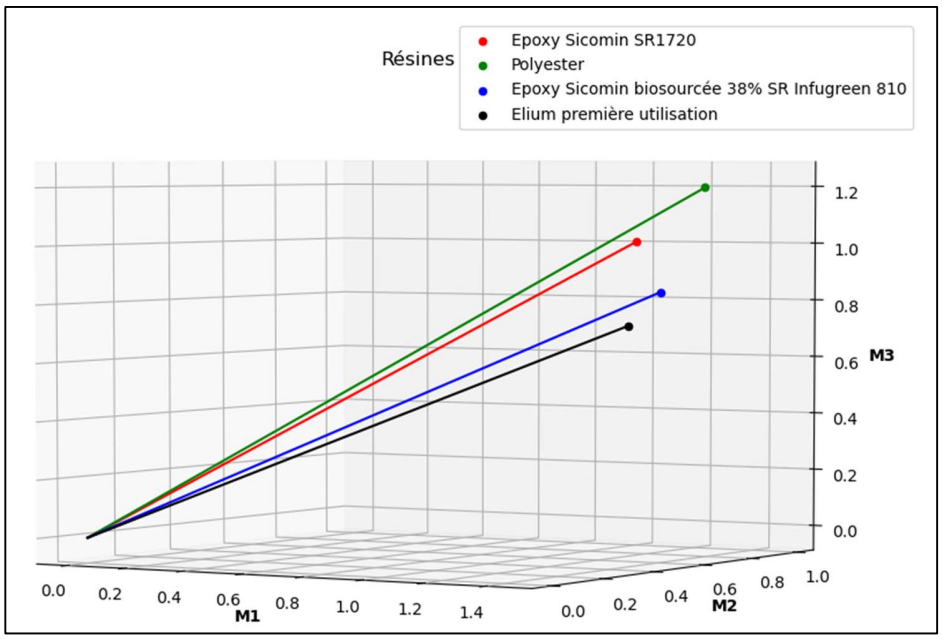

Figure 1.4 3D plot of resins performance indexes

Thanks to their low GHG emissions, flax/hemp fibers have the lowest M3 values. What's more, flax fiber is the one of the latter two that minimizes M1 and M2, so it's the best candidate. Aramid fiber (Kevlar) would also have been good, but its cost in SM$ is too high (120 SM$/kg). Finally, Elium® resin is the best candidate from the outset. What's more, its thermoplastic nature makes it recyclable. So, its M3 index (its environmental impact) decreases with each recycling and reuse if recycling is less energy-consuming than production (lack of data on this subject).

Arkema's Elium® resin and flax fiber were thus chosen. For the hull sandwich material, foams made from recycled PET were selected. Finally, vacuum resin infusion was chosen as the best compromise between environmental impact and part performance.

1.2.4 Material mechanical testing

As a follow-up to the preliminary choices made, a mechanical testing campaign was carried out on the flax / Elium® composite. The aim was to obtain engineer's constants for the characterization of the material's ply, so that it could be implemented in finite element models via laminate theory. It also validates the use of the infusion process for manufacturing.

ASTM D3039 and ASTM D3518 are used to measure the uniaxial tensile and shear behavior of the composite, respectively. The test specimens are made using the same process chosen for the hull construction: vacuum infusion. Plates are made first then cut to the right dimensions. A peel-ply fabric is placed on both sides of the plate to even out the surface appearance. It should be noted that this resin requires an assembly leak rate of less than 1 mbar/min, beyond which zones of non-polymerization of the resin may appear at the air inlets. In addition, the vacuum must be maintained at a vacuum pressure of less than 0.9 bar, as the resin contains a solvent which vaporizes above this limit, causing the assembly to boil and incorporating porosities into the composite. Here, it is set at 0.7 bar, as this is the maximum value to ensure that the vaporization pressure is never reached locally in the vacuum bag. Elium® resin is therefore a very special resin to use.

The dimensions and weights of the sheets allow us to calculate an average composite density of 1178 kg/m3 To calculate Poisson's ratio and shear modulus, bi-directional strain gages are glued to some of the specimens, as shown in Figure 1.5.

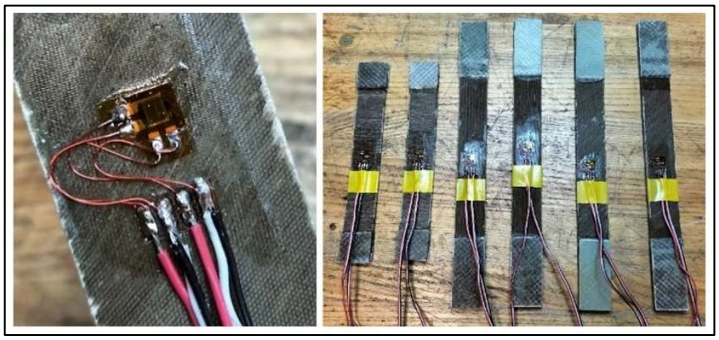

Figure 1.5 Wired strain gauge (left)/ Specimen set (right)

Table 1.2 summarizes the observations made on the failure mode of the various specimens in accordance with ASTM D3039. Table 1.3 groups results of the calculations to determine engineer's constants of the material.

Table 1.2 Failure modes of flax / Elium® tensile specimens

Test	Tensile 0°	Tensile 90°	Tensile $\pm 45°$
Failure mode according to ASTM D3039 (*type / area / location*)	SAM (Long. Splitting / At tab / Middle)	LVV (Lateral / Various / Various)	AGV (Angled / Gage / Various)

Test	Tensile 0°	Tensile 90°	Tensile $\pm 45°$
Image			
Observations	Longitudinal breaks over the entire length	Inter-fiber matrix fracture	Progressive fracture in single plies or groups of plies

Table 1.3 Results of mechanical tests on flax / Elium® composite

Lot	v_f	Quantity	Value	Std dev
UD 0°	34,90 %	$E_1\ [GPa]$	18,41	1,6
		$R_{m,1}\ [MPa]$	221,26	31,1
		$A\%_1$	1,19	0,08
		ν_{12}	0,41	
UD 90°	38,00 %	$E_2\ [GPa]$	3,56	0,22
		$R_{m,2}\ [MPa]$	14,76	0,92
		$A\%_2$	0,44	0,05
		ν_{21}	0,07	
UD +/-45°	33,90 %	$E\ [GPa]$	5,09	0,36
		$R_m\ [MPa]$	61,72	5,48
		$A\%$	2,76	0,57
		$G_{12}\ [GPa]$	1,6	

It is then possible to compare the specific properties of the composite studied with another, more "conventional" composite. Preliminary tests carried out on glass/epoxy specimens (E_1=38.3 GPa, R_(m,1)=789.9 MPa, density 1.9) show that the longitudinal stiffness and specific tensile strength of the flax/Elium® composite are 78% and 45.5% respectively of those of the glass/epoxy composite. The recyclable bio-composite is therefore almost as good in terms of stiffness, but half as strong.

Other tests have also been performed during the design phase to validate the manufacturing processes and assembly methods for the hull, namely:

- Bleeder holes spacing tests: to select the best compromise between lightweight and no dry spots during resin infusion.

- Peel tests: to verify the bonding between flax / Elium layers ant the recycled PET foam core.
- Pull through and bearing tests for bonded metallic inserts into the deck: to quantify the strength and select the threaded inserts according to the load they have to carry.
- Resistance test for the anchor point of cunningham and vang pulleys.

1.2.5 External and internal design

The hull geometry is created using CATIA V5 software and its surface design module. It is based on a wireframe "skeleton" comprising the shapes of the deck, the centerline of the hull and several sections of the hull. Its surface is then generated using the software's various surface creation tools. Figure 1.6 shows an overview of the hull shape.

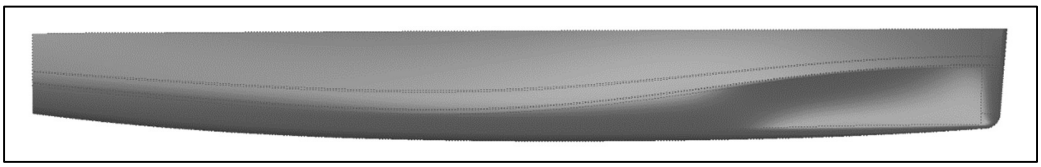

Figure 1.6 Hull shape of Rafale IV

Overall, the hull is very thin and slender, as is the case with all foiling Moth hulls today. This makes it easier to glide at low speeds, and therefore easier to take off on the foils. The lines are smooth to limit both hydrodynamic and aerodynamic drag. Concave shapes are visible at the front of the hull. They are inspired by current AC40 hulls. The hull rises slightly from the last third of its length to reduce the stall zone of the boundary layer and facilitate air penetration. This also limits the amount of material and therefore the weight of the hull. In terms of dimensions, the overall length is 3330 mm, the beam width 400 mm and the height 370 mm. This ensures compliance with class rules.

The deck of the Rafale IV hull is quite simple. Overall, it is flat, with recesses to allow wings to be inserted flush with the upper surface once installed. It features a bulb at the front to lend cross-sectional inertia to this area, which is highly stressed in bending.

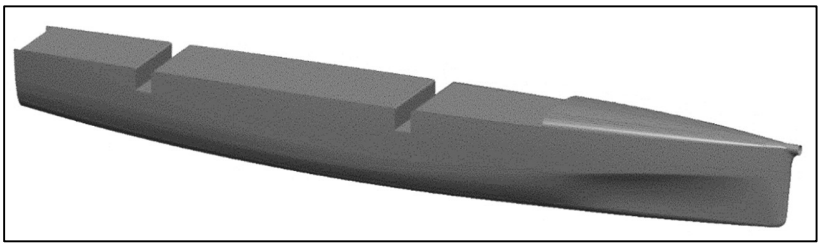

Figure 1.7 Deck and hull of Rafale IV

SuMoth regulations require the boat to be unsinkable with an 85 kg skipper. If we consider a 50 kg rigged boat, we have according to Archimedes' buoyancy expression the equation:

$$V_{depl} = \frac{P_{tot}}{\rho_{eau} \cdot g}$$

$$V_{depl} = \frac{(50 + 85).9{,}81}{1000.9{,}81} = 0{,}135\ m^3$$

The hull must therefore have a minimum volume of 135 liters to comply with the regulations. The total volume of the hull is 339 liters. The buoyancy constraint is therefore largely respected. This volume places the waterline at around one-third of the hull, with a skipper weighing 70 kg.

Once the outer shape of the hull has been determined, its internal structure can be designed. This enables the hull to withstand the various local and global loads to which it is subjected, while preventing its cross-section from deforming and thus limiting the risk of buckling. We can locate the main loading zones on the boat's hull, which will be the areas to be reinforced with bulkheads. These areas are shown in Figure 1.8.

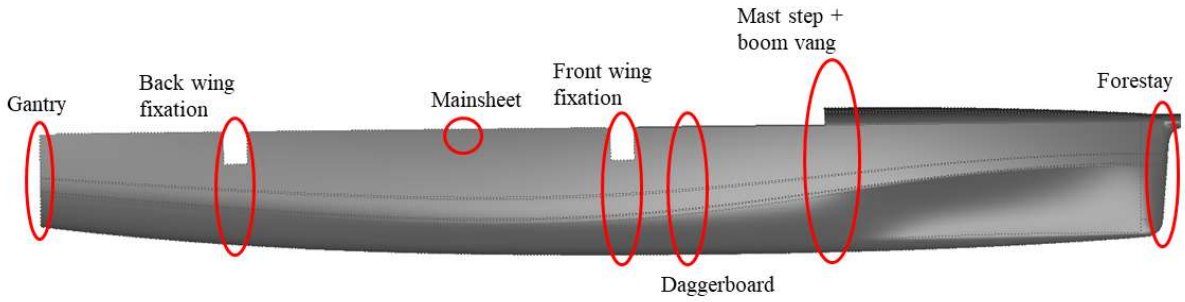

Figure 1.8 Main loading areas of the moth hull

To decide the longitudinal positioning of elements (wings, mast, foils, etc.), mass distribution has also been considered to guarantee a good pitch stability of the boat and the ability of the skipper to control it without having to go further than the wings area. It has been performed using our DVPP to validate this condition in many sailing configurations.

The addition of the ship's structural and equilibrium criteria results in an internal structural geometry for the hull. This is shown in Figure 1.9.

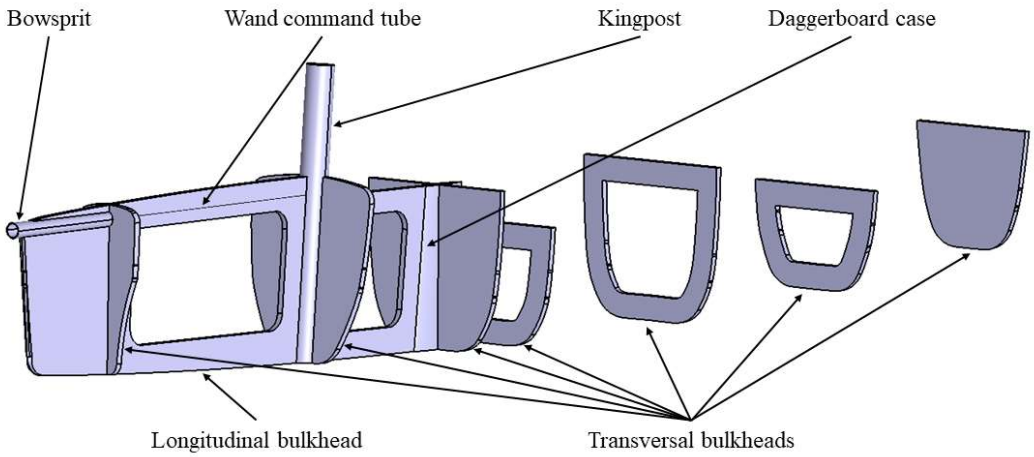

Figure 1.9 Internal structure

1.2.6 Structural design with FEM

Once the hull geometry has been defined, the next step is to dimension the hull structure. This enables us to define the scantlings required to support the loads applied to the hull while sailing. To do so, finite element modelling is used with the Hyperworks software from Altair. Both linear static and linear buckling analysis are done. The failure criterion for these simulations is Puck's criterion. It is chosen according to the advices of the article *Recommendations for designers and researchers resulting from the world-wide failure exercise* (Soden, Kaddour, & Hinton, 2004).

After meshing the geometry with shell elements and defining the contacts and the materials as we can see in Figure 1.10, two main different load cases are studied:

- Load case 1: Fully loaded sailing case. The moth is sailing right with its rig loaded at maximum tension (forces from the rig are the most critical).
- Load case 2: Righting situation after a capsize. The moth floats on its side and the skipper tries to right it by standing at the end of the daggerboard to unstick the sail from the water.

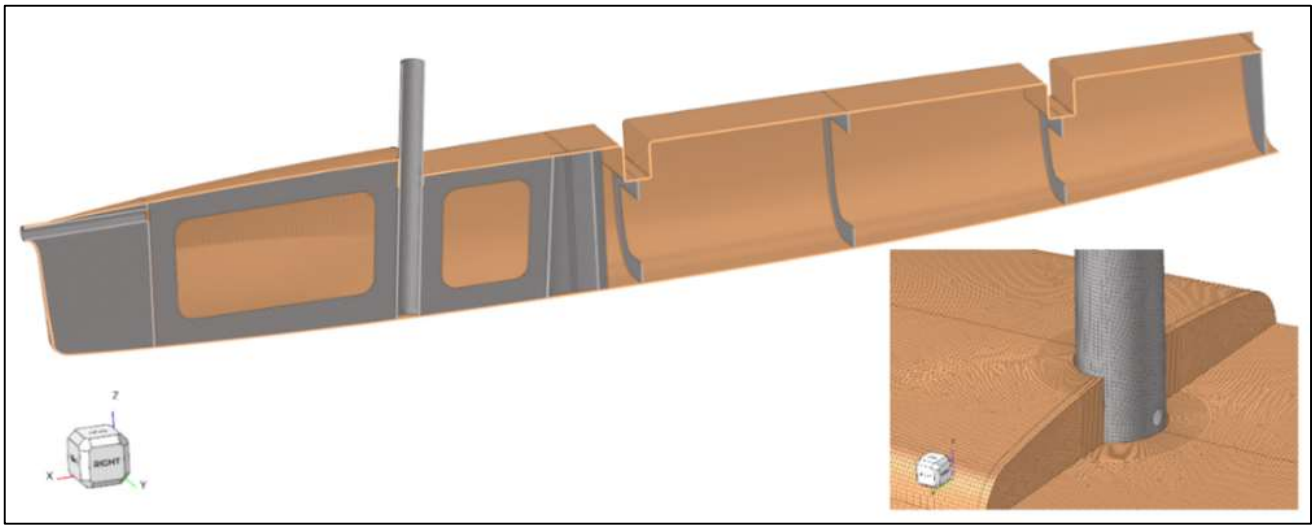

Figure 1.10 Cross-section of hull structure mesh and detail of mesh around mast step

Details about applied loads and failure criterion results can be found in APPENDIX A. Both analyses show that the safety factor of 1.2 is respected with the chosen laminates. It reaches its minimum values around the kingpost are goes up to 4-5 in the less stressed areas. However, it is important to keep a sufficient thickness of composite in these areas because it has to resist to the skipper's heels when using the boat or righting it. The deck also has to resist to local loads coming from the deck fittings. Secondary finite element analysis show that the safety factor is about 1.25 for a heel hitting the hull and 1.7 for the tension of the rig attached on the deck. To finish, there is no buckling risk under the applied loads. Scantlings are consequently validated. Carbon fiber is only put in the most stressed areas at the front of the hull which have to support high rig loads.

Laminates for the hull can be summarized by the following points:

- 2 plies of flax / Elium each side of a 6 mm recycled PET foam core for the hull.
- 2 plies of flax each side of a 12 mm recycled PET foam core for the deck (high density in the areas of the threaded inserts).
- All bulkheads behind the daggerboard are 3 plies of flax /Elium each side of a 12 mm recycled PET foam core.
- All bulkheads in front of the daggerboard are 3 plies of carbon / Elium (recyclable) each side of a 12 mm recycled PET foam core.
- Bowsprit and kingpost are carbon / epoxy filament winded tubes.

All of this makes a carbon fiber content by mass of 4% and a total theoretical mass of 18 kg for the hull.

1.3 Gantry

The gantry used for Rafale III was not structurally strong enough, leading to breakage on several occasions. So, for Rafale IV, we needed a new, stronger gantry. To achieve this, we abandoned the tubular design and opted for a shell gantry, to improve strength and aerodynamics. What's more, the design is improved by the fact that the part is continuous with the boat's hull. The gantry has a fairly common shape, compared to recent Moths. In our case, it is in two parts : a U-shaped shell, which closes towards the end, and a flat plate bonded to the top to close the whole. This choice was made to limit the complexity of the manufacturing process with the tools available to us.

Figure 1.11 General shape of the gantry

The U-shaped curve of the gantry is identical to the end of the boat's hull, to ensure continuity and ease of assembly. The dimensions were chosen to comply with the regulations (total length: 450mm). The end of the gantry is fitted with a vertical carbon tube for connection to the rudder.

A finite element study was carried out. This showed the failure zones. The zones highlighted are the stress concentration zones. This allows us to see where to apply carbon strips for reinforcement. As for the rest of the gantry, it's made of a combination of unidirectional and bidirectional (woven) flax fibers surrounding a thermoformed recycled PET foam.

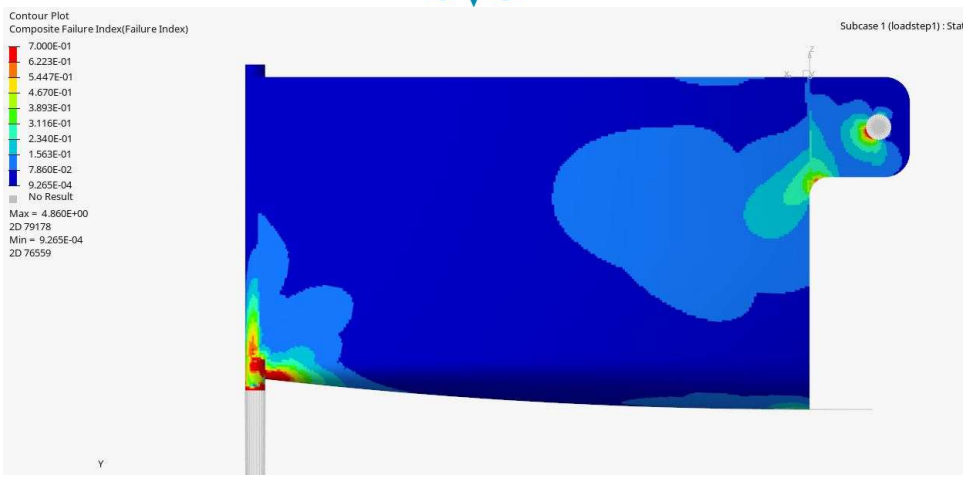

Figure 1.12 : Results of the FEA for the gantry

The gantry contains a total of 1.55 m2 of carbon fiber, equivalent to 14,1% of its theoretical mass of 2,2 kg.

1.4 Hydrofoil system

The Rafale 3 moth has shown stability issues during previous competitions. Specifically, the rear wing of the hydrofoil system was too lifting, causing the sailboat to pitch forward. It was decided to completely revise the hydrofoil system to improve its hydrodynamic performance.

In addition to the hydrodynamic aspect, the team observed that the junction between the wing and the rudder was prone to breaking. This issue must be fixed to ensure more reliable flight.

Finally, the rudder and daggerboard of Rafale 3/3.5 were manufactured using molds from an old catamaran's daggerboard. These molds result in a chord length that is too large compared to existing moth daggerboards. Therefore, the generated drag is deemed too high.

1.4.1 Design requirements analysis

Hydrodynamic requirements

For the performance targets of the boat, the requirements are based on information gathered during the Sumoth Challenge 2023. Several discussions were held with professional skippers. In general, the use of two sets of wings is required. The first set consists of large wings for moderate winds, allowing the sailboat to take off at 7 knots. The second set comprises small wings for strong winds, enabling takeoff at 9 knots. The Rafale sailboat must be able to take off in any wind condition, hence the 7 knots speed used for design. During the 2023 edition, a speed sensor was installed on Rafale 3.5, showing that the sailboat could sustain flights of several seconds at a speed of 18 knots, with a peak of 20 knots recorded. Therefore, the wing systems must minimize drag at its cruising speed of 18 knots. Additionally, for safety, the sailboat must still be able to fly adequately if the speed reaches 25 knots. The wing system must always generate adequate lift to support the boat. The boat's mass is approximately 50kg, and the current skipper's mass is about 70 kilograms (dressed). The lift must slightly exceed the boat's mass to lift it. A force of 1,200 newtons is required for takeoff. In flight, the boat has an estimated

heeling angle of 20 degrees. The lift must then exceed by a factor of 1/cos(20). A force of approximately 1,300 newtons is therefore necessary. Table 1.4 summarizes the sailboat's speed and lift requirements.

Table 1.4 Summary of the requirements for the performance part

	Speed [m/s]	Lift [N]	Lift ratio on the main wing [%]
Take-off	3.6	1200	80
Flight	9.3	1300	90

Structural requirements

Two criteria must be met for structural verification. The first criterion is the mechanical strength of the hydrofoil system in the event of an accident. And the second criterion is the deformation of the system during standard flight.

For the deformation part, the daggerboard must not deform excessively to allow proper flap operation. A maximum deformation of 10 millimeter during flight is tolerated. R. Ponter's study shows that a daggerboard can withstand a deflection of approximately 60 millimeters if a point force of 500 newtons were applied to its tip.

The daggerboard can experience two extreme loading cases. Firstly, the "Nosedive" (Figure 1.12), which occurs when the Moth pitches forward. It is then abruptly decelerated, largely by the water drag force on the daggerboard. To determine this force, the daggerboard is considered as a flat plate being pulled through the water.

The second accident scenario occurs when the daggerboard provides too much lift. Only half of the daggerboard supports the boat's weight. This generates a significant moment of force on the daggerboard.

The daggerboard must be able to withstand the "Capsize" accident (Figure 1.12 :Figure 1.12). This accident occurs when the boat abruptly turns sideways. As before, the boat is abruptly decelerated. But in this case, it is the daggerboards that must bear the load. Figure 1.12 presents the defined loading values for each accident scenario.

Figure 1.12 : Extreme loading cases: "Nosedive"[1] on the left and "Capsize"[2] on the right

[1] Extrait de https://www.storerboatplans.com/foils/sailing-hydrofoils/foiling-week-2018-part-1-composites-and-foils-sydney

[2] Extrait de https://www.sail-world.com/Australia/Moth-Worlds

Table 1.5 Summary of mechanical strength requirements

	Extreme deformation on flight [mm]	Extreme pressure [Mpa]	Extreme load [N]
Wings	10 (With 1300N lift)	0.031 MPa (On the wing area)	1200 (at one quarter of the wingspan)
Shafts	60 (with 500N applied to the tip)	0.035 Mpa (On the shaft area)	-

1.4.2 Optimization programs

To determine the key parameters of the hydrofoil system, optimization programs are coded. The purpose of these programs is to find values that enable the boat to fly efficiently while adhering to the deformation and strength criteria imposed by the design requirements.

Hydrofoil Wings

For the wings of the hydrofoil system, the objective is to find dimensions that minimize drag during flight (wingspan, chord, etc.). Prandtl's lifting-line theory connects several formulas that approximate drag given lift, the wing profile, and various geometric dimensions of the wing. The theoretical principle involves taking aerodynamic data from a 2D profile (of infinite length) and transforming them into 3D data (finite length) based on the wing's geometric dimensions. Drag and lift can then be calculated based on the wing's angle of attack. Optimization is divided into two separate resolutions, one concerning the daggerboard wing and one concerning the rudder wing.

Daggerboard wing program

The optimization program tests several wing configurations and outputs the dimensions and installation angle that minimize drag during flight. Figure 21 shows the various parameters sought by the program. Note that the flap percentage is determined at cf/c = 0.30. This choice is made based on existing literature, where this ratio typically ranges between 0.27 and 0.33. Similarly, the taper ratio of the wing is determined at λ = ct/cr = 0.3.

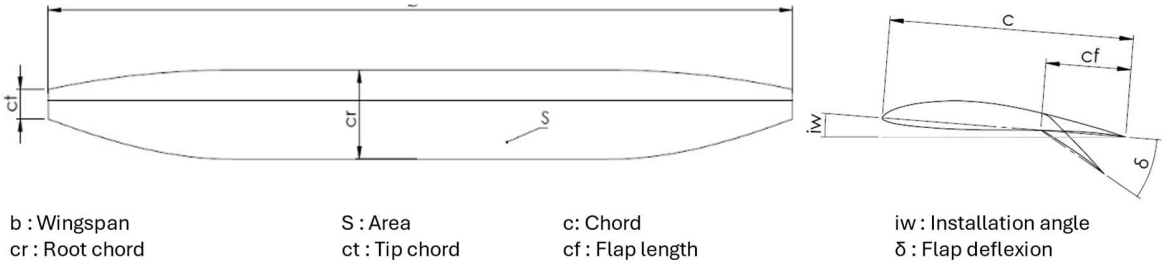

Figure 1.13 : Main dimension of the daggerboard wing

The results obtained are presented in the Table 1.6. One important point to note is that for each profile, the results are very similar. The drag force in flight is always close to 55N. The profile that generates the least drag is the NACA6409 profile with a drag of 53N. It is also noted that it is

always the maximum wingspan that generates the least drag. This is because approaching an infinite wing length reduces drag. However, for manufacturing and structural reasons, the wingspan is limited to 100cm. The installation angles (iw) vary considerably between the different wings. For example, the NACA 63-412 profile has an angle of 6 degrees, which approaches the stall angle. In comparison, the angle of the FX76-MP-120 profile is 2.6 degrees, giving it more freedom before stalling. CFD simulations need to be performed for these configurations to validate these assumptions.

Table 1.6 Values of optimization results for the daggerboard wing

N°	Thickness ratio t_c [-]	Area S [m2]	Wingspan b [cm]	Installation angle i_w [°]	Flap deflexion (flight) δ_{fl} [°]	Flap deflexion (take-off) δ_{to} [°]
NACA4412	0.12	0.079	100	5.1	-10	25
NACA6409	0.09	0.079	100	3.6	-10	25
FX 76-MP-120	0.12	0.079	100	2.6	-10	25
Eppler 393	0.12	0.081	100	4.5	-10	25
NACA63-412	0.12	0.082	100	6.0	-9	25

Rudder wing program

The rudder wing does not have a flap. However, the rudder wing can change its angle of attack during flight (trim). Generally, a significant angle of attack is required during takeoff. Once the Moth is in flight, the skipper quickly decreases the angle of attack. The optimization program for the rudder wing provides the dimensions of the wing that minimize drag during flight. The image below (Figure 2-5) shows the various dimensions to be determined. The profiles used for the resolution are standard low-camber NACA profiles. Low camber profiles are chosen because the rudder wing must generate less lift than the daggerboard wing. The resolution program is based on the same principle as that of the daggerboard wing, with only the variables changing.

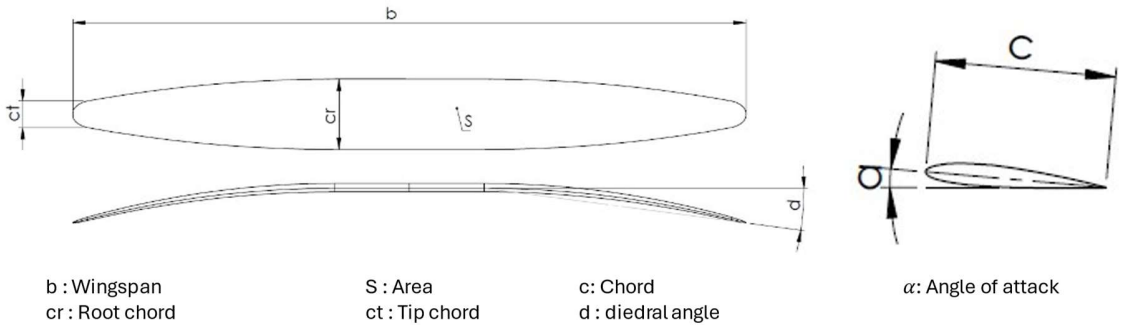

Figure 1.14 : Main dimension of the rudder wing

The results obtained are presented in Table 1.7. As with the daggerboard wing, the drag results are close, ranging between 9.6 newtons and 10.4 newtons. Therefore, this selection criterion may not necessarily be the most relevant. Thin profiles generate less drag, but their manufacturing is more complex. Due to their thin sections, their surface inertias are lower, resulting in lower

mechanical resistances. Additionally, a large wingspan is preferable to reduce drag. This large wingspan increases the lever arm of the pressure, leading to higher wing stresses. For these reasons, it is decided to select the NACA 1412, which has a thicker profile.

Table 1.7 Values of optimization results for the rudder wing

	Lift (flight) L_{fl} [N]	Drag (flight) $\boldsymbol{D_{fl}}$ [N]	Finesse ratio(flight) f_{fl} [-]	Lift (take-off) L_{to} [N]	Drag (take-off) $\boldsymbol{D_{to}}$ [N]	Finesse ratio (take-off) $f_{déc}$ [N]
NACA0006	130	33.2	3.9	240	9.6	24.9
NACA0009	130	34.5	3.8	240	9.8	24.4
NACA0010	130	35.6	3.6	240	10.1	23.8
NACA1408	130	33.2	3.9	240	9.8	24.6
NACA1410	130	36.0	3.6	240	9.9	24.2
NACA1412	130	37.7	3.4	240	10.4	23.0

CFD analysis wings validation

To confirm the previously found results and finalize the profile selection, several CFD simulations are conducted. For each profile, takeoff and flight configurations are tested.

To verify the daggerboard wings, four simplified wings are modeled in 3D. Each wing has one of the profiles to be tested. The wing consists of a constant section at the root and the previously mentioned taper. The dimensions of each wing (area, chord, wingspan, installation angle) are chosen based on the optimization results. The flap is connected to the wing without interruption of material. Its deflexion angle can be adjusted according to the chosen flight condition (takeoff or cruise). For the rudder wing, only one wing is modeled in 3D, featuring the selected profile (NACA1412). The wings are then imported into the Star-CCM+ software. A fluid domain is created around the wing to simplify solver calculations, and the wing is meshed symmetrically. Appropriate meshing is applied (Figure 1.15).

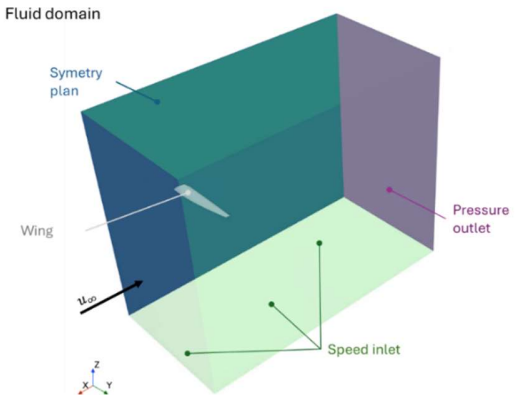

Figure 1.15 : Fluid domain

The lift generated by the daggerboard wing according to the CFD is then lower than the predictions of the optimization calculations (Table 1.8). This is particularly evident during takeoff,

with a decrease of approximately 20% compared to the desired lift. The results for the different wings are still very similar. However, the FX 76-MP-120 profile shows excessive lift during flight. This would require increasing the flap angle to create more downforce, thereby increasing drag as well. For the rudder wing, the results are close to the expected ones.

Table 1.8 CFD results for the daggerboard wing

Main wing			Take-off	Flight
Desired lift		[N]	960	1170
Eppler 393	Lift	[N]	820	1 050
	Drag	[N]	80	50.0
	Finesse ratio	[-]	10.3	21.0
FX 76-MP-120	Lift	[N]	734	1 580
	Drag	[N]	82	64
	Finesse ratio	[-]	9.0	24.7
NACA 6409	Lift	[N]	758	1 098.0
	Drag	[N]	74	50.0
	Finesse ratio	[-]	10.2	22.0
NACA 4412	Lift	[N]	760	932
	Drag	[N]	72	50
	Finesse ratio	[-]	10.6	18.6

Finally, the Eppler 393 profile is selected. This profile exhibits good lift during takeoff. Additionally, the thickness of this profile is higher, facilitating manufacturing and increasing wing strength. To compensate for the lack of lift during takeoff, the surface area is increased to 0.09 square meters. And the takeoff angle is modified to 30 degrees of deflection. A final CFD analysis is conducted with these new dimensions (Table 1.9). The lift in flight is then too low. This indicates that the flap angle (currently at 10°) should be reduced to around 9 degrees of deflection, resulting in a decrease in drag. Ultimately, the glide ratio during takeoff is 8.3 and the glide ratio in flight is close to 18.9. For the rudder wing (Table 1.9), the results are close to the optimization results. Therefore, the wing is kept with its current dimensions.

Table 1.9 CFD results for the two wings

Rudder wing			Take-off	Flight
Desired lift		[N]	240	130
NACA 1412	Lift	[N]	268	128
	Drag	[N]	11	40.0
	Finesse ratio	[-]	24.4	3.2

Daggerboard wing			Take-off	Flight
Desired lift		[N]	960	1170
393 Eppler (version finale)	Lift	[N]	944	1 022
	Drag	[N]	114	54.0
	Finesse ratio	[-]	8.3	18.9

Hydrofoil shaft optimisation

For the daggerboard, the optimization primarily focuses on the structural aspect. The goal is to have a sufficient chord and profile thickness to ensure strength. However, the objective is also not to oversize the daggerboard to avoid unnecessarily adding weight and generating excessive drag. The code calculates the displacement generated by the force (F) and the safety factor of the daggerboard when pressure (p) is applied. The code utilizes laminated composite theory and outputs the stiffness matrices "ABD" and compliance matrix "abd" based on the material and laminate. It also returns the Failure Index (inverse of the safety factor) based on the required moment of force per unit length.

Compared to the new loading requirements, the laminate of Rafale 3 $[(0,25,0,0,-25,0)_6]_s$ remains very conservative (Figure 1.16). For a laminate composed entirely of carbon fiber, the number of plies could be reduced. The daggerboard of Rafale 3 has a chord of 20 centimeters at the root. This dimension could also be decreased. At the time, existing molds from Rafale 1 had been used. However, these molds had been made for a catamaran. The chord lengths of most Moth daggerboards are generally shorter than 20 centimeters. Finally, the decision is made to opt for the laminate ($[(0,0,0,0,30,-30)_3]_s$) that includes basalt . Carbon reinforcements will be added to ensure rigidity. The chord is chosen at 16 centimeters with a profile thickness ratio of 0.16. This still provides a good safety factor compared to the maximum loading case (Figure 1.16). Additionally, choosing a relatively high thickness ratio allows for space to accommodate various internal elements within the daggerboard (core and wand system).

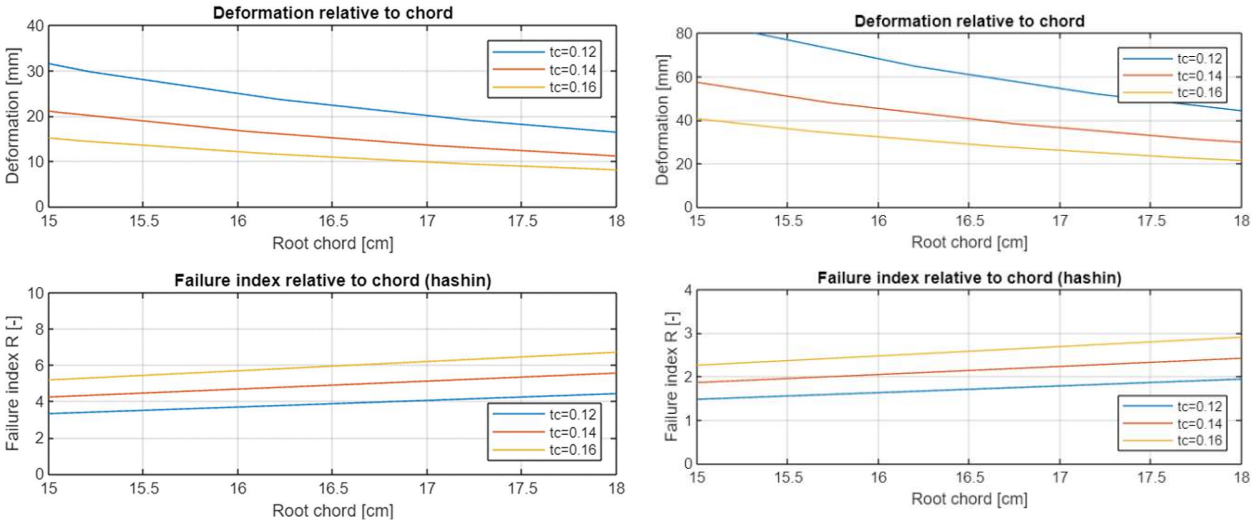

Figure 1.16 : Optimization results of the shaft, carbon laminate (right image) and basalt laminate (left image)

1.4.3 Hydrofoil design

The optimization results provide the overall dimensions of the hydrofoil system. It remains to define the design choices that allow for the assembly of the different parts together. These choices are influenced by both structural and hydrodynamic aspects, as well as manufacturing considerations. Structural and hydrodynamic simulations are conducted to validate the design choices.

Elements junction choice

Two design choices still need to be made. Firstly, the connection between the daggerboard and the foil must be designed. Secondly, the connection between the flap and the foil must be determined. It should be noted that the connection between the rudder and the rudder structure is retained. This system has proven itself in various competitions. It is easy to manufacture, and assembly remains straightforward.

For the connection between the daggerboard and the foils, the goal is to design a removable connection. This allows for future changes of the foils without the need to remake the daggerboards. Two different designs are proposed.

1. Carbon-reinforced bulb manufactured with the foil
2. Metallic connecting piece(s)

Although the first solution is often used by Moths, it is the second version that is chosen. This version has several advantages. Firstly, manufacturing in metal (aluminum) reduces the use of carbon. As a reminder, the use of carbon should represent a maximum of 50% of the mass of the hydrofoil system, and the goal is to minimize its use. Furthermore, the metal piece system can be manufactured for the old Rafale 3 foil. This foil can therefore be reused if needed. Finally, a metal junction provides satisfactory strength in this area, which is often prone to breakage.

For the connection between the flap and the foil, solutions shown in Figure 1.17 are proposed:

1. Connection with a flexible kevlar hinge
2. Connection with a metal axle
3. Connection with metal hinges (Rafale III)

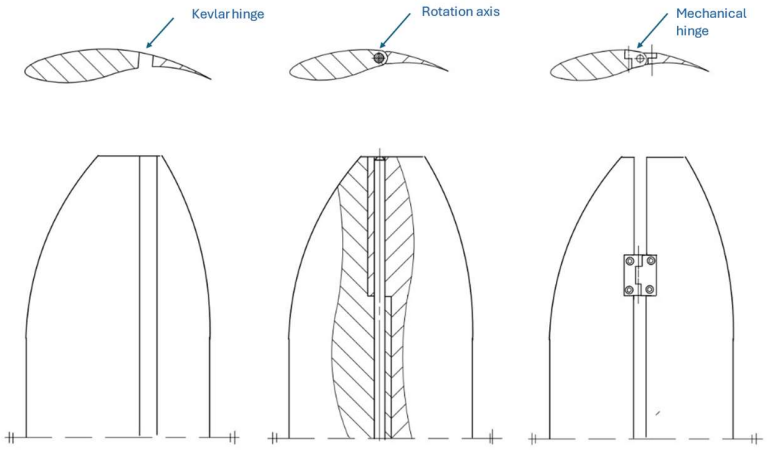

Figure 1.17 : Sketch of the proposed solutions for the wing-flap connection

Solutions 1 and 2 have the advantage of not creating too large of a gap between the foil and the flap on the upper surface. This ensures continuity of the flow, leading to increased hydrodynamic performance. The solution of a rotating axis is complex to manufacture. The rotation axis needs to be guided along the entire length of the foil. Consequently, high coaxiality is required over a long distance. Additionally, the skins at this location would be too thin. The solution of a kevlar skin is ultimately chosen. However, there is little documentation explaining the manufacturing of kevlar fiber hinges. This lack of information adds a challenge to the manufacturing process. The final CAD design obtained is presented in Figure 1.18.

Figure 1.18 : CAD of the hydrofoil system of Rafale IV

1.4.4 Hydrofoil FEM validation

Only simulations for the front part of the hydrofoil system are conducted (daggerboard and daggerboard foil). This section receives more load than the rudder part. The rudder part will be manufactured with the same number of plies as the daggerboard part and will have a higher safety factor. In the future, a more detailed analysis could be conducted on the rear rudder to minimize weight. The software Altair is used for the simulation. Structural analyses are separated into studies. Firstly, the shaft is analyzed independently. Then, the entire hydrofoil system is analyzed.

Structural analysis of the shaft

Three loading cases are conducted on the shaft. The first case assesses the stiffness of the shaft when subjected to a force at its tip. The second case validates the strength of the shaft under extreme pressure due to an accident. Finally, the last case validates that the skins are not at risk of buckling.

To avoid overloading the report, meshing assumptions and discussion of the various results are presented in the appendix. Two important points emerge from this. Firstly, the rudder exhibits a good safety coefficient (factor = 2) under extreme accident conditions. Secondly, the risk of skin buckling is very low. Ultimately, the simulations have allowed for a reduction in the use of carbon fiber by replacing it with basalt fiber.

Structural analysis of the hydrofoil system

Next, the entire hydrofoil system is analyzed. Two loading cases are applied. Firstly, the pressure experienced by the wing in flight is applied to verify that the wing does not deform excessively so that the flap remains functional. A second accident case is tested to validate that the wing and the metal junction do not fail in an accident. As with the shaft, detailed results are found in the appendix. The conclusions are that the wing is sufficiently rigid to ensure proper flap operation. Additionally, the entire hydrofoil system has a good safety factor.

More detailed information about finite element modelling and analysis of the hydrofoils can be found in APPENDIX A.

1.4.5 Validation of the hydrofoil system through CFD analysis

A final CFD verification is conducted to ensure that the connection of the wing to the hydrofoil system does not significantly decrease lift or increase drag. The same assumptions and principles used for the wing alone are applied. The difference lies in the CAD. The vertical stabilizer as well as the connection system are added. The connection system is meshed in the same manner as the wing to gather maximum information at that location. The vertical stabilizer, on the other hand, is meshed with the generic mesh of the fluid domain. Its impact on the wing is less significant.

The results show, during takeoff, a loss of lift of 8% and an increase in drag of 12% for the vertical stabilizer wing. For the rudder wing, the differences are minimal. This implies that the boat will need to go slightly faster to reach takeoff, with an estimated speed of 7.3 knots. For the flight configuration, the lift is minimally affected by the addition of the junction parts. However, the drag is significantly increased for the vertical stabilizer wing with a 20% increase. This decreases the overall finesse of the hydrofoil system from 12.2 to 8.9. Nevertheless, this result remains higher than the finesse of the old vertical stabilizer wing estimated at 5.6.

Figure 1.19 provides a clearer visualization of the effects of the junction parts on the flow. In this figure, the additional drag generated by the junction parts is visible. However, this increase is very localized and does not influence the rest of the wing and the rest of the vertical stabilizer. It is noteworthy that the effects at the wingtip are easily noticeable.

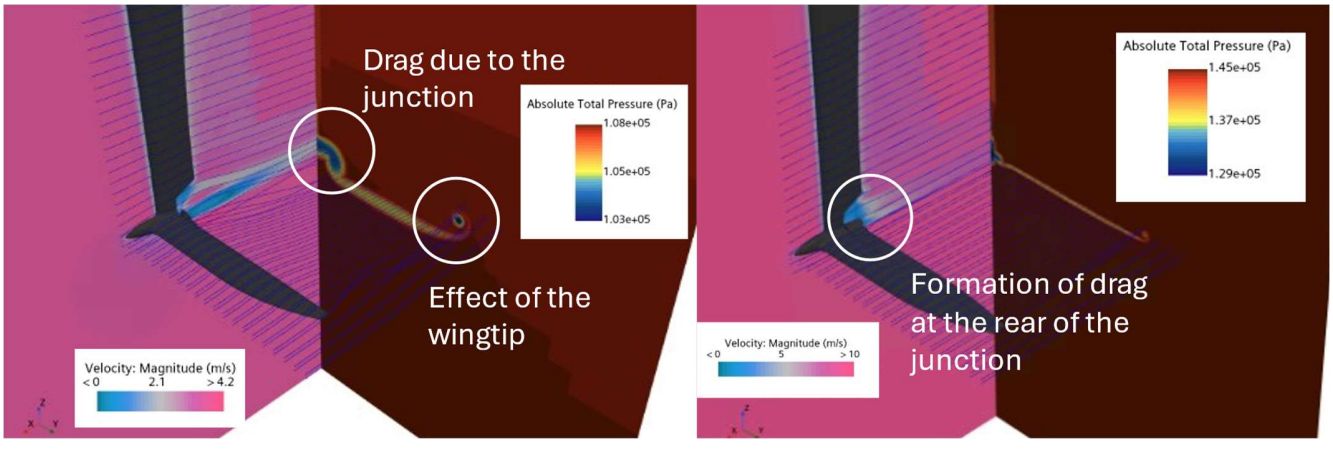

Figure 1.19 : Visualization of CFD results (takeoff on the left and flight on the right)

1.5 Wand

Over the past two years, the club has sailed R3 and R3.5 with the same wand system. The numerous sailings revealed various design and manufacturing problems. The lack of adjustability of the different wand settings quickly became an issue in the optimization process. So, for the new iteration of our moth, it was decided to redesign the wand to make it stronger, more ecological and more reliable.

1.5.1 Design requirements analysis

The new wand must be high-performance, economical, and robust, while being durable and environmentally friendly, and allow stable, controlled flight, whatever the sailing conditions encountered. It must also comply with class rules and not affect the boat's performance. Finally, the system must be easy to repair and dismantle.

1.5.2 Optimization programs

An optimization program was generated using MATLAB software. It was used to find various key system parameters, while ensuring compliance with the design criteria requested by the club. The results thus obtained enable us to obtain the navigation characteristics shown in Figure 1.20.

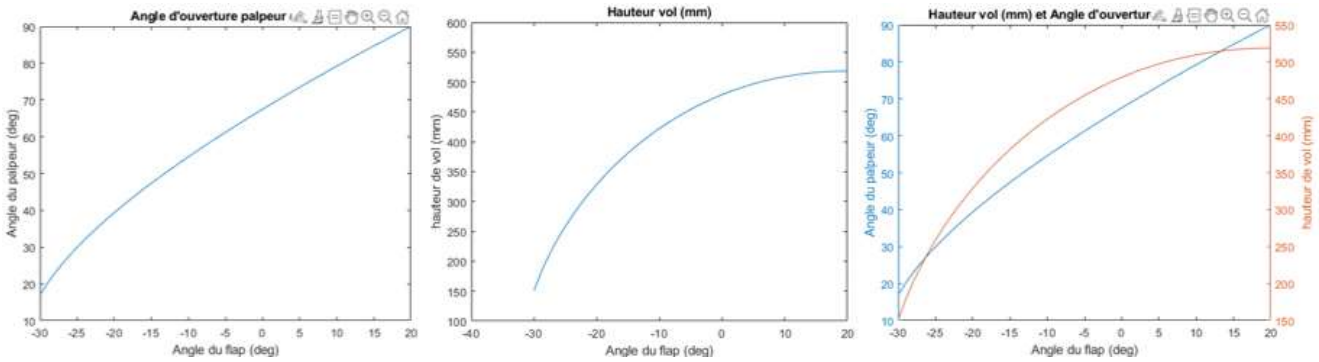

Figure 1.20 - Wand angle [°] as a function of flap angle [°] (left), flight height [mm] as a function of flap angle [°] (center), wand angle [°] and flight height [mm] as a function of foil wing angle [°] (rigth)

1.5.3 Design

Various fittings have been designed to allow the skipper to easily adjust various settings of the wand system. These are illustrated in Figure 1.21 below.

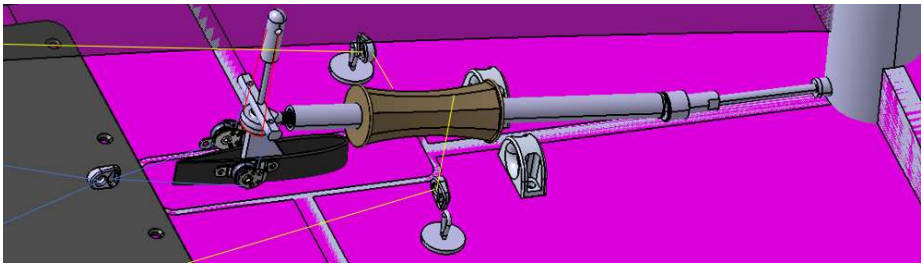

Figure 1.21 - Front section of R4 deck

The red and blue lines in Figure 1.21 above represent the cords used to modify the length of the connecting rod-crank mechanism at the top of the daggerboard. The red lines represent an elastic cord forcing the connection to increase the length to its maximum. This length is then reduced to the desired length using the cords represented by the blue lines. In addition, the yellow lines represent the adjustment for changing the length of the connecting rod. All these controls are passed on to the skipper, who can easily make the various adjustments.

The system used to control the change in wand height has been taken from that on R3 and R3.5. The rope for this adjustment is controlled from the bow of the yacht's deck and is then connected through various parts of the system to the upper part of the wand. The use of elastic cord, represented by the red lines in figure 12 below, enables the length of the wand to be set back to its initial length if required.

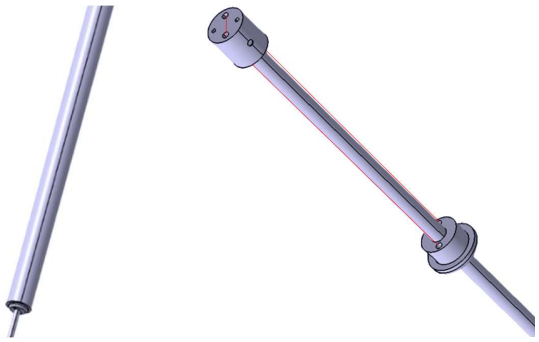

Figure 1.22 – Outside (right) and inside (left) tube of the wand

The subassembly of the wand and bowsprit at the front of the sailing dinghy has been designed to be limited to 450 mm to maintain a 50 mm clearance with the maximum length imposed by the class rules. The complete system assembly looks like this:

Figure 1.23 - Complete R4 wand system

1.5.4 FEA

A structural analysis was carried out on the sub-assembly of the bowsprit and the part connecting the wand to the bowsprit. Unlike the other parts of the system, it will have to survive the application of stresses of different magnitudes in extreme cases. The one with the highest probability of occurrence is a nosedive at a speed of 30 knots. This extreme case generates a

force of 1200 N on the bowsprit. A safety factor of 1.3 has been taken into account. The results obtained are shown in Figure 1.24 below.

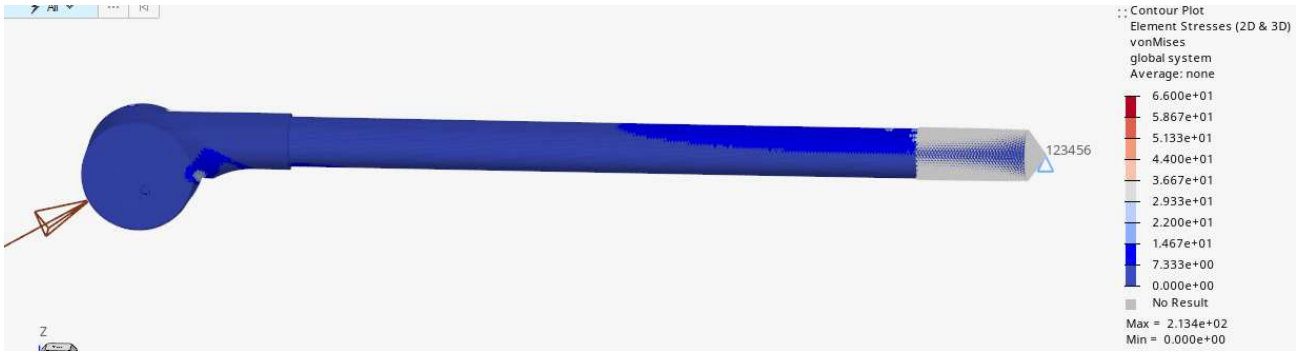

Figure 1.24 – Results of FEA on the bowsprit

1.6 Wings

The wings are the same as last year (flax + Elium resin around a recycled PET foam core). We changed the clips on the four corners. The clip design is virtually the same as last year. The only change is the creation of a hole to accommodate the male part. Most of the work consisted in designing the molds for the fasteners, since we had to make a mold that corresponded to the "forged" composite manufacturing technique, was easy to unmold and reusable. We introduced nuts into the mold to allow a screw to be inserted during unmolding, and to facilitate extraction of the part.

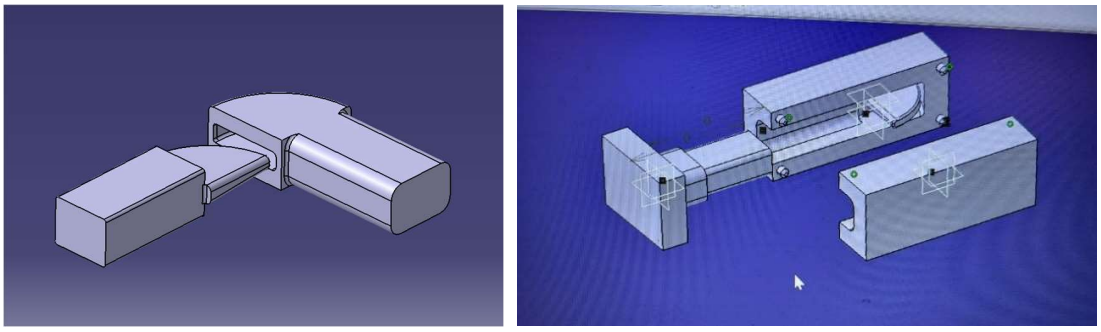

Figure 1.25 New fittings (left), fittings molds (right)

1.7 Rig

1.7.1 Mast step

The mast step is an essential component for connecting the hull of a boat to its mast. In this project, the challenge was to design a mast step that would fit a new hull while reusing the mast from the previous year. The objective was to enable the mast to be adjustable in inclination to accommodate different types of sailing.

The mast step was designed using Catia, with two parts featuring a spherical contact surface to model a ball joint. Acetal, a type of nylon, was chosen as the material for these parts, offering a good balance between mass, friction coefficient, and durability. Additionally, a central piece

made of stainless steel was added to guide the installation of the mast step. To ensure the strength of the mast step, finite element analysis was performed. The main force was estimated to be 1.5 tons at a 45-degree angle, created by the tension of the boom vang. This estimation helped verify the adequacy of the mast step's design to withstand these loads.

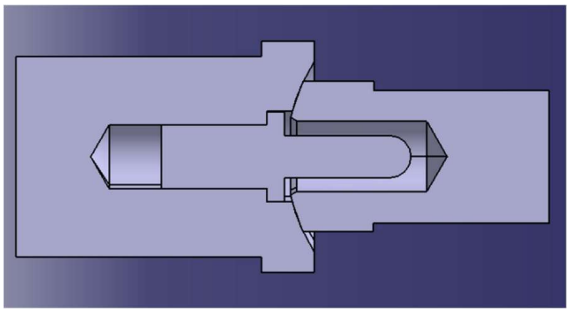

Figure 1.26 Mast step CAD

1.7.2 Vang Lever

The vang lever was an essential addition to our boom to create more tension in our sail. After last year event, the team realized that there was a lack of tension in the sail which made controlling the sail much harder and did not allow us to use our sail to full power. The first step in designing the lever was to find how much force would be applied to the part. It was estimated that 1.5 tons was in the vang.

Thus, the force exerted of the lever was calculated for 3 scenarios: at 90° and ±5°. This gave of a maximum charge of around 13.5 KN at 95°.

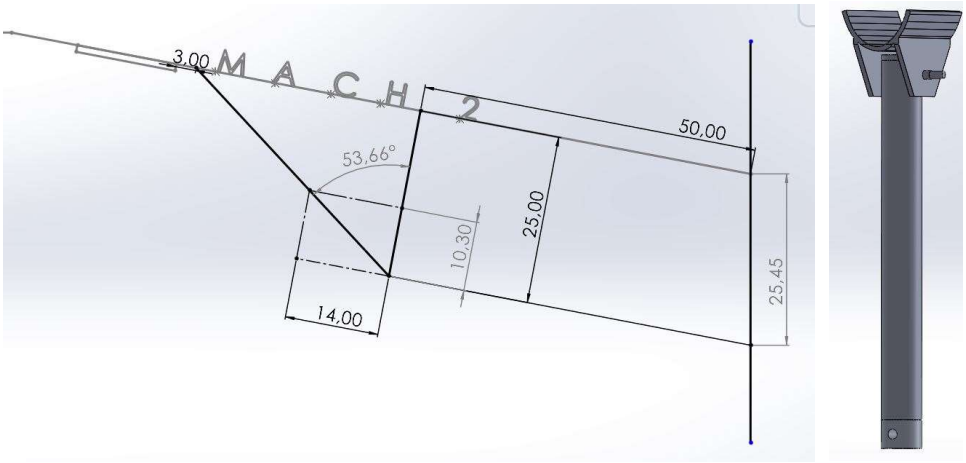

Figure 1.27 Schematic representation of the forces applied to the lever (left) and lever CAD (right)

Once the calculations were done, we researched what was done on the actual market to get some ideas. The team decided to do this in 2 main parts: lever attachment and a lever strut.

The lever will be under an enormous amount of force. Therefore, we implemented 3 different strategies to avoid any failure. First, we decided to make the lever in prepreg carbon fiber to make sure that this critical part had a uniform resin and fiber content. We also decided to add metal inserts to the lever to redistribute the force applied in the holes for the pin.

Figure 1.28 Metal inserts

Finally, for the lever we did two FEA analysis to confirm that our calculations and design ideas were compatible. First, we did analysis of the lever strut because that is where most of the load is applied. Then we did an overall analysis of the sub-system to make sure that all 3 components (strut, attachment, and pin) could support the load. We simplified the lever attachment to simplify the analysis. We realized that not a lot of force was applied in zone A, thus adding them to the FEA analysis does not significantly affect our result. The results confirmed that our design could sustain the amount of force applied to the sub-system.

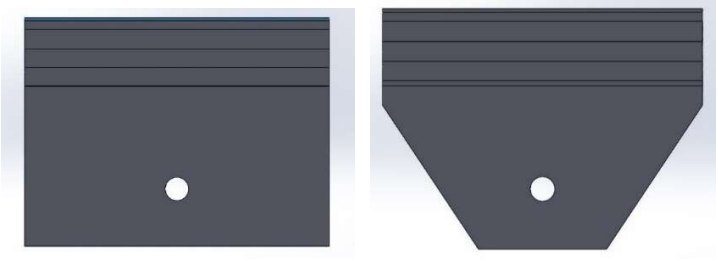

Figure 1.29 CAD for analysis (left), CAD for manufacturing (right)

1.7.3 Spreader

For RAFALE IV, we embarked on designing and constructing a completely new spreader, prioritizing enhanced ecological characteristics and superior performance. These changes were necessitated by the need to harmonize with the boat's new design and rectify the deficiencies of the previous spreader.

The pivotal change in this spreader's design is the reorientation of the bar. Previously, the spreader was fixed in conjunction with the sail, resulting in suboptimal geometry where the bars exerted uneven forces on the shrouds. Consequently, determining the length and angle of the bar became the paramount challenge this year, crucial for achieving an optimal spreader placement to uphold the shroud's integrity.

Figure 1.30 Spreader CAD

1.7.4 Deck fittings

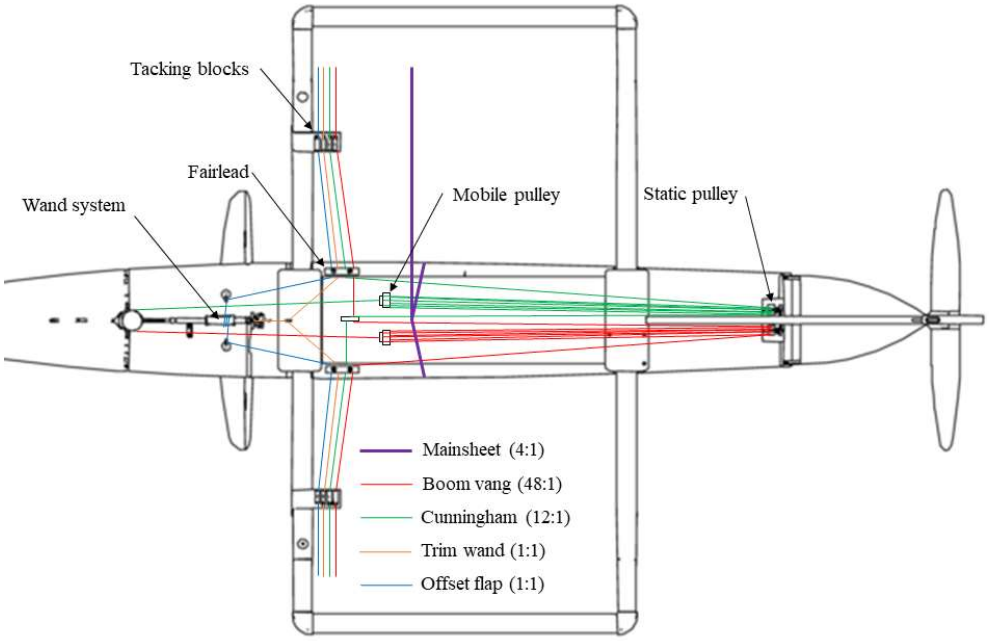

Figure 1.31 Deck fittings

The deck fittings for Rafale IV are shown in Figure 1.31. The control system is symmetrical from port to starboard, so the skipper has access to all settings whatever the boat's point of sail. The movable pulleys of the vang and cunningham are positioned in line with the deck. This gives them more travel and therefore a wider range of adjustments to adapt the sail shape to the conditions. The wand and flap adjustment lines carry very little load.

1.8 Electronics and data acquisition

The onboard system is left more or less unchanged since the revision of last year on the side of the design. We use a Raspberry Pi as the base module in charge of the processing of all the data and it is powered by a generic USB battery. The original plan was to reuse the Raspberry Pi 3 B + from last year but it changed after the received data from the pinout was deemed unusable

due to damages from the moisture while in storage. So, a Raspberry Pi 4 B is used instead. All the data is stored locally in the Pi and can be retrieved once a user is able to access the onboard Wi-Fi module of the Pi. A schematic of Raspberry Pi 4B can be found in Appendix A.

The pi receives data from the GPS module (ZED-F9P GPS-RTK HAT) through a generic serial link using a baud rate of 38400 with a parity bit. The module is powered directly by the Pi using the 5V and ground pinout. The accelerometer/gyroscope module (BNO085) is also directly connected to the Raspberry Pi but instead of using a generic serial connection it is using the i2c protocol. It is also powered by the Pi using the 3.3V and the ground from the available pinout.

All the electronic components apart from the antenna of the GPS are stored within a box rated IP67. The seal of the box from the previous year was irreparably damaged so a new one from the same fabricants was bought as a replacement.

1.9 Performance prediction with a DVPP

As part of the Rafale IV hull design work, a DVPP was developed using the Matlab programming language. This is a simplified version quite similar to that developed in (Findlay & Turnock, 2008). It takes into account the dynamics of the boat only on its longitudinal axis and adds the counter-heel angle parameter not considered in (Findlay & Turnock, 2008). Furthermore, in this model, the expressions for the hydrodynamic and aerodynamic drag of the boat's hull are based on full-scale experimental measurements by Beaver & Zseleczky (2009) on foiling Moths carried out later in 2009. Pseudo-static equilibrium (the boat not being stationary, but in a steady state) is calculated on the vertical axis to determine the flight height, and also in roll and pitch to determine the sail trim and skipper position required to balance the boat. The equations considered in this tool are as follows:

$$m_{tot}.\overrightarrow{a_{bat+skip}}.\vec{X} = \sum \overrightarrow{F_{ext\to bat+skip}}.\vec{X}$$

$$\sum \overrightarrow{F_{ext\to bat+skip}}.\vec{Y} = 0$$

$$\sum \overrightarrow{F_{ext\to bat+skip}}.\vec{Z} = 0$$

$$\sum \overrightarrow{M_{ext\to bat+skip}}.\vec{X} = 0$$

$$\sum \overrightarrow{M_{ext\to bat+skip}}.\vec{Y} = 0$$

To construct this version of DVPP, which does not integrate the boat's dynamics according to the six degrees of freedom, a few assumptions are made.

- A constant load distribution on the foils is considered (modeled by a percentage of the load taken by the daggerboard foil, the rest being supported by the rudder foil. This is a correct approximation in the constant-speed flight phase, but less so in the take-off phase. Boegle et al (2012) detail that in the take-off phase, the daggerboard foil supports 60% to 70% of the boat's load, compared with around 100% at nominal speed.

- The boat's flight height is fixed at the start of the program. As a result, no information is provided on the boat's take-off phenomenon. The boat is considered to be in flight at the height set by the user, as long as the balance of forces permits.
- The angle of heel is set at the beginning of the program as a sailing constant. In reality, the skipper varies it according to the points of sail taken by the boat, in order to optimize performance on the water. For example, he will be more counter-geared upwind to limit drift than downwind, where it is less important.
- The sail's center of buoyancy is assumed to be fixed, whatever the sail's settings. However, this is a reasonable assumption. "The center of effort of sail force is relatively constant until the craft becomes overpowered at which point increasing amounts of luff tension help the leech of the sail to open and 'twist off' thereby reducing the height of the center of effort." (Findlay & Turnock, 2008).
- The drift phenomenon is neglected. The boat's speed vector is assumed to coincide with its longitudinal axis.
- The wave drag generated by the foils is neglected in the calculation. It is small compared to the shape drag and induced drag of the foils.
- The tool we've developed enables us to collect a range of information useful not only for predicting the boat's performance, but also for positioning components such as foils, wings and mast, as well as force values. This data is particularly useful for the design of the Rafale IV hull and hydrofoil system.
- Firstly, the DVPP can be used to plot the boat's polars for different true wind speeds and orientations, as shown in Figure 1.32. Here we can see the maximum speeds attainable, as well as the Moth's flight ranges (true wind angles and speeds allowing take-off) thanks to the abrupt speed changes on the curves.

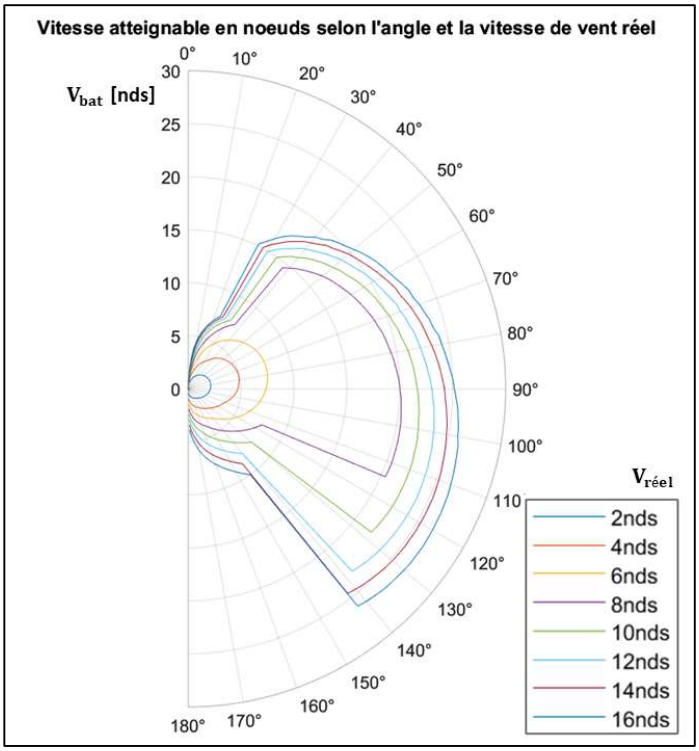

Figure 1.32 Example of polar plot

This program also enables us to check the longitudinal position of the skipper on the boat, which is necessary to obtain balance when the Moth is in flight. This is important because, as the skipper is heavier than the boat, the position of his center of gravity on the boat has a major impact on overall balance. Figure 1.33 shows how the position of the boat's center of gravity influences the position of the skipper, leading to equilibrium.

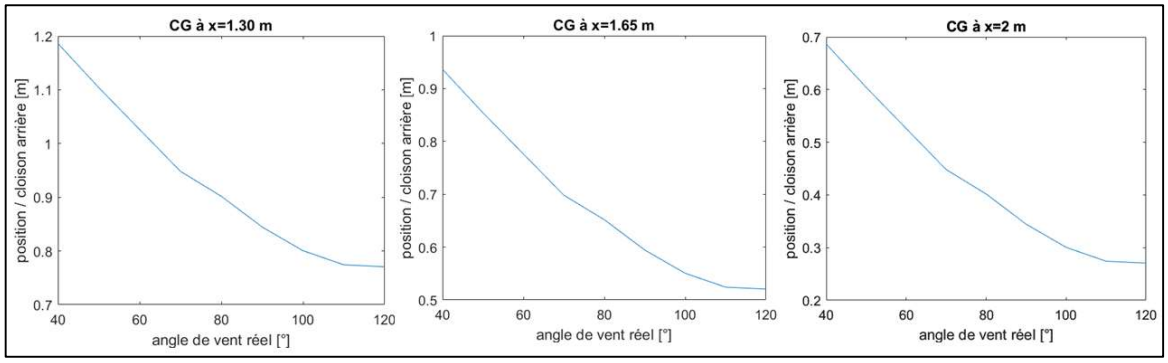

Figure 1.33 Influence of the boat's CG position on the area used by the skipper

As the boat's center of gravity moves towards the front of the hull, the skipper has to hold onto the rear of the hull to maintain balance. To facilitate this, it is preferable to have the center of gravity slightly aft of the daggerboard foil. It's also worth noting that on upwind points of sail, the skipper should move towards the mast and back downwind. This is consistent with the behavior observed when sailing a Moth.

Finally, it is possible to determine the Moth's take-off time and speed for a given orientation and wind speed (take-off calculated at 7.8 knots for a real wind of 12 knots oriented at 50° to the boat's axis), or to analyze the various friction components. It shows that, once the boat has been launched, the aerodynamic drag is the second biggest source of friction after the sail. It's easy to see why professional skippers put so much effort into fine-tuning the aerodynamics.

The study of these different data in relation to the boat's design parameters enables choices to be made for the design of the hull and the boat as a whole. It will then be interesting to compare the theoretical results with the boat's polars under real navigation, plotted using the acquisition system to be installed on the boat. In this way, the model can be fine-tuned and become more accurate.

2 MANUFACTURING AND COST ANALYSIS

2.1 General description

For the Rafale IV prototype, most of the elements are completely rebuilt, namely:

- Hull
- Hydrofoils (verticals and horizontals)
- Wand mechanism
- Gantry
- Spreader

However, some parts could be reused or upgraded:

- Wings have the same structure than last year but with reinforced joins in the corners and some elements added for the rig.
- Boom is upgraded to a more modern design with a one design vang lever to increase the efficiency of the boom vang.
- Some parts of the wand are reused from Rafale 3.5
- The rig is redesigned but most of the ropes, tacks, pulleys, etc. are reused from the last prototype. The sail and mast are the same as last year.

Furthermore, the design of the foils and the gantry is made in such a way that we can reuse the old rudder ant the old wing for the main foil.

2.2 Hull

In this section are presented the projections for hull manufacturing. This includes the molds and also the hull infusion and assembly. Details about the material quantities we planned to use are described in the table at the end of this chapter with the SU$ associated. More details and images about the manufacturing process will be given in the S2 report.

2.2.1 Hull molds

The large-scale 3D printing process was chosen to produce the molds for the Rafale IV hull. The process's ecological credentials (recyclability) and its potential viability for industry were motivating factors in the decision to embark on trials.

The machine used to manufacture the hull molds, shown in Figure 2.1, is a robotic arm mounted on a linear rail, which can be fitted with either a print head or a machining head developed by the Dutch company CEAD. The printing bed is heated, and the whole unit can print or machine parts in an envelope measuring around 3 m by 1.50 m by 2 m. The plastic granules are fed to the extruder via a system of pipes connected to a dryer (the granules must have a certain moisture content before they can be printed) and a pump. The whole system is controlled by a touch-sensitive control panel.

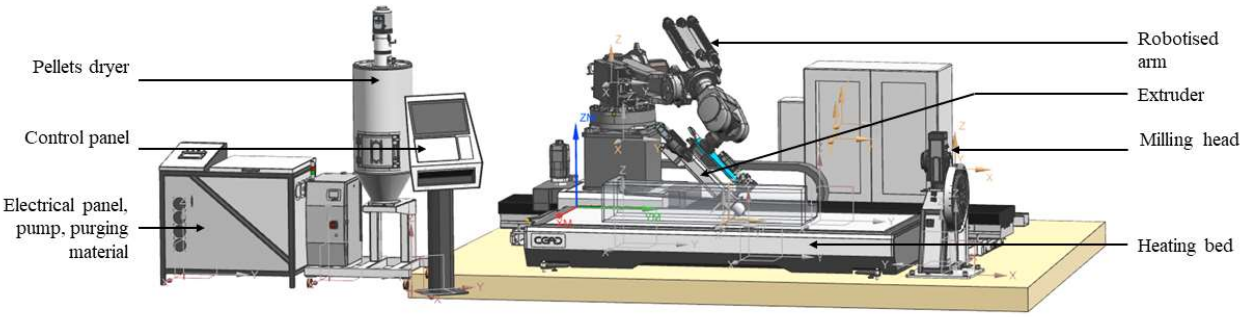

Figure 2.1 CEAD AM Flexbot robot and its environment

The hull mold is shown in Figure 2.2. It is a large parallelepiped block in which the external shape of the hull is hollowed out. Its dimensions are 3650 mm by 700 mm by 470 mm. The counter-

molds for the bonding lips are shown in light gray. One of them is transparent to reveal the inserts molding the wings slots in orange. The useful surfaces are the top surface, which is used to position the counter-molds and inserts for the bonding lips and the vacuum bag, and the inner surface, which gives the hull its shape. They must therefore be machined to remove the irregularities caused by the printing beads.

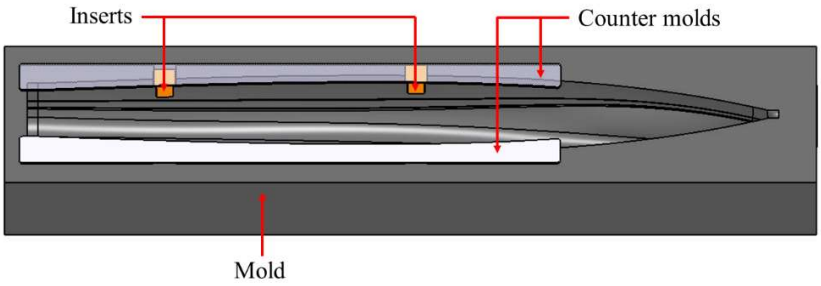

Figure 2.2 Hull mold CAD

Tests have shown that slicing along a 45° plane and printing along a helical path are the best ways of limiting part deformation due to cooling. In this way, we can take advantage of the part's cross-sectional inertia. This greatly reduces the deformation observed, thus avoiding problems of material shortage during machining. For the same reason, and to confer rigidity to the mold, it is chosen to print with the largest diameter nozzle available (18 mm). For reasons of layer time (between 70 and 100 s for the selected plastic) and machine envelope, the mold is printed in four parts, then bonded. Printing layers are then removed by machining the useful surfaces of the mold. It is done at a specialized company because no machines are large enough at ETS. The deck mold is manufactured using the same process.

The material selected for 3D printing the molds is granulates of recycled polyethylene terephthalate (PET) reinforced with 30% glass fiber. This choice is justified by the fact that PET is one of the few plastics with which Elium® does not react. Indeed, this resin tends to dissolve most of them. What's more, our supplier produces this material by recycling plastic from the oceans and industrial waste. Such molds can be recycled at ETS using a shredder and a machine which remakes granulates from the previously processed plastic so that molds of the next prototype could be made from the exact same material.

2.2.2 Infusion, assembly and finish

Once the molds are ready, they are covered with a PTFE film to ensure proper unmolding and all plies, the core and consumables are placed into them. Then the resin is infused with a partial vacuum pressure (specific to the Elium resin) and, after polymerization, the parts are unmolded. The bulkheads are cut with a CNC router. Everything is bonded together with a methacrylate adhesive which molecular structure is similar to the Elium resin. This ensures a better bonding and recyclability. Hand laid wet layups are made to finish parts junction. The finish is done with polyester fairing putty and a classic boat paint is used to protect the natural fiber composite from humidity as well as giving a good look to the boat.

2.3 Gantry

For the gantry, the mold manufacturing process is identical to that for the boat hull: 3D printing using recycled PET. This is followed by a machining stage to make the mold's functional surfaces usable. The useful area of the mold is then covered with PTFE film to enable unmolding. Finally, the part is infused. This choice was made to meet our objectives of reducing our environmental footprint, and also, enable us to rapidly obtain the mold with a controlled technique.

2.4 Hydrofoil system

2.4.1 Daggerboard shaft and rudder shaft

For the shaft, the optimization results show that carbon can be replaced by basalt. It is then largely made with this fiber. Some carbon reinforcements are still added to ensure rigidity. The decision is made to manufacture the rudders using the infusion technique. The FEM software predicts that the Carbon fiber represents about 54% of the fiber mass used. This shows that the percentage of carbon will be well below 50% of the total mass of the shaft. The requirements are largely met. The process allows the use of a thermoplastic acrylic resin (Elium resin) from the company Arkema. This resin has the advantage of being recyclable.

The shaft comprises a total of 20 plies of dry fiber. No infusion had yet been done with so many plies over such a large surface. To ensure the production of the shafts, it is decided to make the molds out of MDF in case the infusion fails. This would allow putting the molds in the oven and carrying out the shafts by reimpregnating. However, this material is not the most eco-friendly. Nevertheless, the molds are reusable for several years by the club. If this infusion succeeds, it would then be preferable, in future designs, to opt for an eco-friendlier mold. For example, the same technique used for the hull molds could be applied.

For manufacturing, the two half-shells are then infused. Two bonding lips, respectively on the leading edge and the trailing edge, are planned in the mold design to allow centering and assembly of the two shells. It is planned to insert a recycled PET foam core inside the two half-shells and glue them together. For the daggerboard, the core must allow the passage of the metal guide rod for the flap. At the top of the rudder, some plastic pieces will be added to accommodate the rudder structure piece. The metal junction piece is finally glued to the bottom of the shaft.

2.4.2 Metal additive manufacturing

The metal parts will be produced using Additive Manufacturing. The parts are then designed accordingly, aiming to minimize the number of supports. Figure 2.3 shows the chosen orientation for the parts and the supports put in place. The parts require machining for functional areas. These surfaces are minimized to reduce machining time. Only the surfaces in contact between the two parts will be machined. To enable this machining, a 1-millimeter layer is added to the printing CAD.

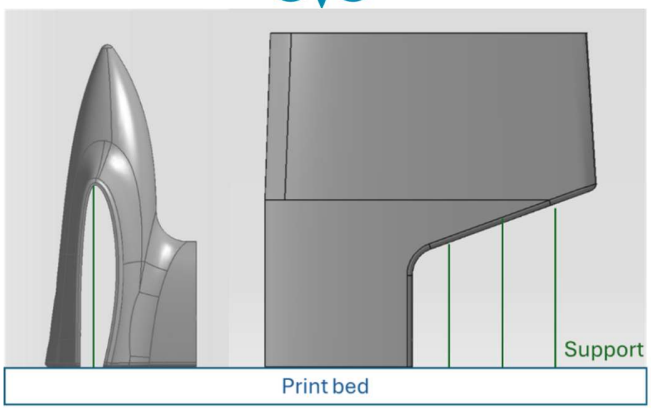

Figure 2.3: CAD drawing of the print bed

2.4.3 Hydrofoils wings manufacturing

The manufacturing of the wings is more meticulous and precise than that of the shaft. The prepreg technique is preferred in this case. The molds are made of aluminum, ensuring the precision of the shape. For the front wing, the extrados surface will be added with the flap attached entirely, allowing for the installation of the Kevlar hinge with a flexible adhesive added in the hinge area. The intrados surface is manufactured separately without the flap part. The counter-mold for the extrados is planned to be machined in aluminum. The one for the intrados is planned to be 3D printed in Nylon 6 reinforced with glass fiber. Both molds have bonding lips. The two molds need counter-mold. They will then be bonded together using structural adhesive. Filling adhesive will be inserted into the wing, providing good shear strength.

The manufacturing process for the rear wing is like that of the front wing, except that the rear wing does not have a flap. Both the upper and lower surfaces extend from the leading edge to the trailing edge. The counter-mold is then unnecessary. Like the daggerboard wing, the wing joint pieces is bonded using structural adhesive. Although carbon prepreg is still used, the fiber CAD show that the percent of mass of the carbon fiber will be approximatively 40% of the wing's total mass. Furthermore, the prepreg used is outdated material from a company dating back to 2018. This utilization helps avoid waste.

2.5 Wand

The spoon used for R3 and R3.5 is reused for the R4 wand, as this part has not caused any problems in use. In addition, many parts are purchased and machined to facilitate assembly.

With 3D printing, more complex, low-stress parts can be manufactured more easily. This led us to decide to print the two parts used to adjust the height of the system's connection to the fin. All carbon parts of the wand are upcycled.

2.6 Wings

The wings are the same as last year. We've changed the material of the fasteners on the four corners. They are made of 50% carbon fiber scrap, 50% bi-directional basalt fiber and Elium resin. We use the “forged” composite technique to manufacture them. The clip molds are 3D printed with PETG.

2.7 Rig

2.7.1 Mast step

The mast step is manufactured using a process of machining on traditional lathes and CNC machines. The materials used for the fabrication are sourced from leftovers from previous projects for 2 out of 3 parts. This helps minimize environmental impact and reduce costs. The mast step designed for this project thus represents an effective and durable solution, allowing for adjustable mast inclination while ensuring good resistance to the loads encountered during navigation.

2.7.2 Spreader

The spreader is manufactured using eco-friendly processes and materials. Firstly, all the composite material in the bar is made with Elium resin, which is recyclable. Additionally, there are five layers of flax fiber for every one layer of carbon fiber. This part comprises three main components, each crafted through distinct processes: the bar, junction plates, and shims. The bars are meticulously crafted from five layers of infused flax fiber and one layer of wet layup carbon fiber, ensuring robustness and resilience. The junction plates not only interconnect the bars but also secure the shroud to the spreader. These plates are meticulously fashioned from the remaining old prepreg carbon fiber, precision-cut using a water jet cutting method. Lastly, the remaining components are plastic parts manufactured through 3D printing. The primary cost driver lies in the 1.5 hours of water jet cutting.

2.7.3 Vang lever

Once the design was finalized, we needed to start thinking about manufacturing our parts in the most sustainable way because most of the parts are out of carbon. For the lever attachment, we 3D printed the mold. Since the boom is symmetrical, we printed both side of the part as one piece to reduce the material used. Furthermore, the fiber used for the wet lay-up is from carbon fiber scrap and the epoxy was expired. We decided to put our wet lay-up under vacuum to have a better fiber and resin ratio. Also, the top part of the attachment will be molded directly on the boom to reduce the number of molds printed and have a better accuracy. For the lever strut we decide to recycle the carbon tube from the compressive bar of Rafale 3 wings. However, the tube was not thick enough. Thus, we used expired pre-impregnated carbon fiber and resin film from leftover scraps. The aluminum inserts will be machined. The insert will be assembled with the strut using a structural adhesive made for nautical use.

2.8 Onboard electronic system

To manage to manufacture the onboard system, we put everything in an IP67 box, reuse the code from last year and adapt it to be used on the newer raspberry PI since some of the interfaces differ. We are also using a new GPS module since the last one broke and reusing the accelerometer/gyroscope from the previous year. Both are connected to the raspberry Pi through the header. To be able to reuse the accelerometer/gyroscope we need to desolder the old GPS module and accelerometer/gyroscope from the stack made for the previous year's system. We then plan to proceed to resolder the accelerometer/gyroscope conversion board to the top of the new GPS hat. The new box is from the same manufacturer as the box from the

previous year. To be able to pass the antenna we drill a hole on the side of the box to make the connector pass and seal the base of it to the box. The box itself is attached to the hull, inside the gantry. The battery is also going to be the same as last year.

2.9 Materials

2.9.1 Elium thermoplastic resin

Elium resin, developed by Arkema, is a thermoplastic resin known for its versatility and sustainability in composite materials. It's a liquid resin that can be used with a variety of reinforcing fibers such as glass, carbon, or natural fibers like flax or hemp. Elium resin offers several advantages including low cure temperature, fast processing times, and the ability to be recycled. It has similar properties than an epoxy. In terms of processing, the Elium resin is specific because it contains a solvent which evaporates at too low vacuum pressures. The resin must therefore be infused under 700 mbar of vacuum pressure. Elium resin parts can be reshaped by heating the composite. It offers new manufacturing possibilities.

2.9.2 Flax / Elium composite

Flax / Elium is a lightweight and recyclable biocomposite. Its density is around 1.2. It is almost as stiff as a glass / epoxy composite but half as strong. Because of the impossibility to wove perfectly aligned flax fibers and the low vacuum pressure imposed by the resin, it is really difficult to obtain above 40% volume fraction of fibers in an infused flax / Elium composite.

Flax absorbs moisture which negatively impacts its mechanical properties so it is really important to add a protective coating on the outside of a flax reinforced composite (even more for a boat).

2.9.3 Carbon / Elium composite

Carbon / Elium composite is similar to a carbon / epoxy one but the thermoplastic resin makes this material recyclable. Parts can be shredded and reformed in a thermocompression tooling or the resin can be separated from fibers and purified to make it reusable in an infusion.

2.9.4 3D printed recycled PET

This material is used to print most of the tooling for the infusion of the boat. It is reinforced with 30% GF in our case. We chose it because PET is one of the few materials which doesn't react with the Elium resin during infusions. Its processing with a large-scale 3D printer requires tests to find the best layer time and temperatures of the extruder. It can be dry machined easily and makes strong molds which are suitable for small-scale production.

At the end of life, parts can be shredded and melted to reform pellets and print new parts.

2.9.5 PET foam core

The core foam we use to produce our parts is a recycled PET foam with a density of 80 or 300kg/m^2 supplied by our partner Gurit. It is an isotropic material which has good compressive and tensile moduli to produce rigid parts.

2.10 Cost analysis

A fictitious currency, SuMoth dollars (SM$), is offered to encourage teams to use sustainable materials and processes. The estimated cost of building the boat must be established and not exceed the maximum budget of 10 000 SM$. The following table details the budget calculation for each item in the table. We have tried to detail the estimated quantities as precisely as possible.

Table 2.1 Cost analysis of Rafale IV

Boat Part	Material and Processes	Amount	Unit	Cost (SM$)
Hull Mold	PET : Recycled	500,00	kg	0
	3D printing	50	h	1000
	Machining (CNC)	24	h	960
Hull	PET	5	kg	100
	Dry fabric Flax	6	kg	0
	Liquid thermoplastic Resin Arkéma Elium (recyclable)	30	kg	0
	Carbon fibers : Std Modulus	3	kg	450
Gantry Mold	PET : Recycled	35	kg	0
	3D printing	4,5	h	90
	Machining (CNC)	4	h	160
Gantry	Liquid thermoplastic Resin Arkéma Elium (recyclable)	1	kg	0
	Dry fabric Flax	1	kg	0
	Carbon fibers : Std Modulus	0,5	kg	75
	PET : Recycled	0,3	kg	0
Hydrofoils Mold	MDF/HDF wood : All	50	kg	1000
	Aluminum: All	2	kg	20
	Machining (CNC)	24	h	960
Hydrofoils	Carbon fibers : Std Modulus	3	kg	450
	Liquid thermoplastic Resin Arkéma Elium (recyclable)	5	kg	0
	Dry fabric Basalt Fibers	2	kg	0
	Aluminum: All	2	kg	20
	CF/Epoxy Prepreg :Epoxy / Std Modulus	0,6	kg	180
	3D printing	42	h	840
	Oven cure	15	h	300
Wand	3D printing	4,5	h	90
	Machining (CNC)	0,5	h	20
	Liquid thermoplastic Resin Arkéma Elium (recyclable)	0,3	kg	0
	Dry fabric Basalt Fibers	0,01	kg	0
	PLA	0,05	kg	0,5
	Element upcycled from R3	0,05	kg	0

Boat Part	Material and Processes	Amount	Unit	Cost (SM$)
Wings	PET : Standard	2	kg	40
	3D printing	30	h	600
	Carbon fibers : Std Modulus (scrap)	1	kg	150
	Dry fabric Basalt Fibers	1	kg	0
	Liquid thermoplastic Resin Arkéma Elium (recyclable)	3	kg	0
	Dry fabric Flax	0,5	kg	0
	Polyester: Lamination (outdated)	0,1	kg	1,5
Mat step	Machining (CNC)	3	h	120
	Stainless Steel: All	0,2	kg	6
Vang Lever	Carbon fibers : Std Modulus (scrap)	0,2	kg	30
	Std. Epoxy : Lamination Resin	0,1	kg	2,5
	PETG	0,1	kg	1,5
	3D printing	1,5	h	30
Spreader	Dry fabric Flax	0,3	kg	0
	Liquid thermoplastic Resin Arkéma Elium (recyclable)	1	kg	0
	PETG	0,1	kg	1,5
	Carbon fibers : Std Modulus	0,1	kg	15
	CF/Epoxy Prepreg :Epoxy / Std Modulus	0,1	kg	30
	3D printing	1,5	h	30
Consumables	MMA Bonding	7	kg	105
	Vacuum bag	50	Unit	100
	Peel ply	25	Unit	125
	Vacuum bagging: Tacky tape	18	Unit	144
	Spiral tube (inf.)	10	Unit	10
	PE vacuum hose	80	Unit	80
	Brushes	20	Unit	40
Other elements	Control System	200	USD	200
	Fittings	200	USD	200
	Ropes	100	USD	100
Forecasted total				8877,5

The projected budget is approximately 8900 SM$ and does not exceed the competition budget of 10 000 SM$. It is interesting to note that the processes (3D printing and machining) account for more than 60% of the total, while the materials represent only 11%. The actual budget in SM$ will be presented in the S2 report to analyze the difference between the projected and actual costs, and to conduct a critical analysis of the use of the fictitious currency.

3 SUSTAINABILITY ANALYSIS

3.1 General description

Based in Montreal, Canada, Team Rafale is traditionally the only non-European team participating in the competition. This unique situation forces our team to use air transportation to travel and transport the boat to Lake Garda. Consequently, logistics put the team at a disadvantage as it starts with a significantly higher carbon footprint compared to other participants. Therefore, at Rafale, we strive to be exemplary in sustainability for the design and construction of the boat. The life cycle approach is truly at the heart of the project, guiding the design and manufacturing processes.

Compared to previous versions, Rafale IV is designed to improve both the overall performance of the boat and its ecological footprint. In this context, almost the entire boat has been redesigned and rebuilt, especially major parts such as the hull, gantry, and foils.

3.2 Boat and elements lifecycle

This section details the sustainable approaches employed in the construction of the fourth version of the Rafale boat.

3.2.1 Design and Rafale III

The life cycle analysis begins at the design phase. The boat is designed to reuse certain parts from the old model that are still in good condition to extend their lifespan and exploit their full potential. The wings, sail, mast, and trampolines from the old boat have been retained. In a spirit of circularity, the new gantry is designed to accommodate the old rudder, while the new foils can reuse the old foil wing in addition to a new, more efficient one.

3.2.2 Molds

In this new version of Rafale, more responsible molds are used. The hull and gantry molds are made by 3D printing, using recycled PET from marine debris and industrial waste. The PET is also recyclable and can be remelted for new prints. These molds can be reused many times; according to our estimate, it is possible to make about thirty hulls from the mold. Therefore, it is entirely possible to amortize the impact of the molds over several years if they are reused for other competitions.

For better precision, the foil mold will be ordered from a supplier. This mold will be machined from fiber panels due to the inability to choose a more responsible material. The molds for some small parts, such as the wings and boom attachments, will be made with the workshop's small 3D printer. Unfortunately, it does not have recycled PET, forcing us to use standard materials such as PLA or PETG.

3.2.3 Composites

The goal for Rafale IV is to make the boat almost 100% recyclable. To achieve this, bio-sourced fibers and recyclable resins will be used to manufacture the various parts. On one hand, flax fibers will be used for the mast, gantry, and spreader bar. On the other hand, basalt fibers will be used for the foils, rudder wand, and wings attachments. These fibers have a very low environmental impact. The resin used, Elium, is like infusion resins but can be recycled multiple times at the end of the hull's life.

MarineShift 360 can be used to validate the sustainability of flax and basalt. By comparing the impact of the hull based on its composition (flax, basalt, and carbon), it can be noted that flax is the fiber with the least impact in most impact categories (climate change, marine eutrophication, mineral resource scarcity, non-renewable energy). Basalt is also better than carbon in all categories.

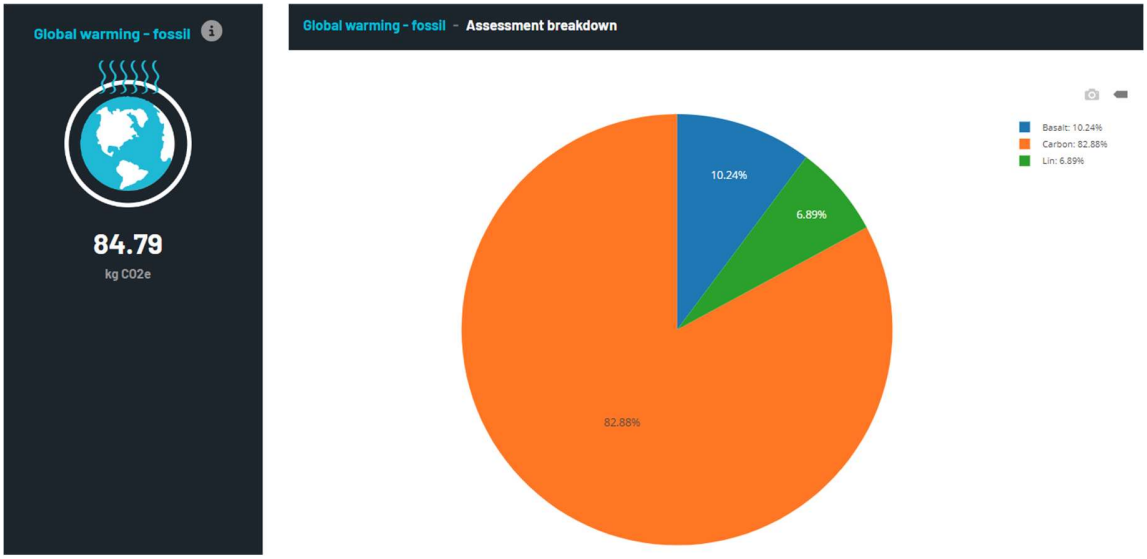

Figure 3.1 Comparison of the impact of carbon (orange), flax (green) and basalt (blue) fibers on climate change

An example comparison of different fibers with MarineShift 360 for climate change impact shows that flax and basalt fibers emit significantly fewer greenhouse gases than carbon fibers. The quantities listed correspond to the amounts needed to make a boat hull (they are not similar for each fiber). However, for the water consumption category, flax fiber has the most significant impact due to the water needed to grow the plant.

3.2.4 Processes and energies

The main processes used are 3D printing, machining, and the use of a vacuum pump for composite infusions. Although these processes are energy-intensive, the advantage of the Quebec energy mix is that it is composed of 99% renewable energy (REC). In the LCA analysis that follows on MarineShift360, renewable electricity from hydropower will be used to represent the Quebec energy mix.

3.2.5 Scraps, Expired and Reused Materials

Other materials from Rafale III that are still in good condition are reused on Rafale IV. For example, the vang is made from an old carbon tube, as is the boom. Some parts of the rigging are also reused.

We also prioritize the use of industrial scraps. We use fabric and carbon fiber scraps for assembling the hull, gantry, wand, and boom. We also have several expired materials, such as methacrylate glue, polyester resin, and prepreg carbon, which are used for the hull, boom, and spreader bar.

3.3 End-of-Life Plan

The combination of recycled and recyclable PET molds with bio-sourced composites offers numerous end-of-life opportunities. The molds can be reused multiple times before being recycled.

The Elium resin in the composites can also be recovered, recycled, and reused. Unfortunately, this process will not benefit our team in the LCA. This resin is used in almost all parts of the boat to give a second life to the elements and consider the positive effects of its recycling, even if it is not beneficial to us now.

Bio-sourced fibers (flax and basalt) are interesting at the end of life because their biodegradability means they have very little impact at this stage of the life cycle. They are also recyclable but cannot be reused for marine applications as they lose their mechanical properties after recycling. However, they remain usable for simpler manufacturing after recycling. We will try to recycle as many fibers as possible.

When it is not possible to reuse or recycle a boat element, it will be sent to a landfill.

3.4 Theoretical LCA

To evaluate its relevance and impacts related to manufacturing, a preliminary life cycle analysis was performed on MarineShift360 for each part. This theoretical LCA was conducted on MarineShift360, and the details are in chapter 5 In comparison, the actual analysis will be presented in the S2 Report.

3.5 Actions for a sustainable future

To reduce pollution, we are convinced that life cycle thinking must be at the heart of all processes. This starts with an eco-design approach, aiming to minimize the use of materials and energy, and to favor bio-sourced materials that have less impact on biodiversity and climate change. Additionally, it is essential to consider the end-of-life of products from the design stage so that each element is recyclable, reusable, or biodegradable.

We also believe that the use of 3D-printed molds with recycled materials for designing parts is a promising way to reduce pollution. If the molds are well maintained, they allow to produce many parts, amortizing the impact of manufacturing. Moreover, 3D printing from recycled and recyclable PET is developing increasingly. Thus, at the end of the mold's life, a large part of it can be recycled to start the process again. This innovative process is still rarely used as few industries have the necessary means for recycling, but it represents a promising solution.

For composites, we suggest using a mix of bio-sourced fibers and recyclable resin. We hope that, eventually, our prototypes will be entirely made with this mix, making the boat 100% recyclable. This innovation is recent and not yet adapted on a large scale. Therefore, we encourage companies to develop it as quickly as possible.

Finally, this applies to all sectors: it is about practicing sobriety. This means minimizing energy, water, and raw material consumption. For example, this can be achieved by reducing the number of test pieces and consumables during infusions. What has the least impact is what we do not consume.

4 TEAM

4.1 Team members

- Augereau, Xavier
- Bailet, Thibaut
- Bazireau, Alban
- Beaumont, Tom
- Bienvenue, Steph
- Blanche, Baptiste
- Bluteau, Karl-Philippe
- Bouchard, Cédric
- Duflos, Nicolas
- Faucher, Jean-Cédric
- Janin, Amory
- Legrand, Quentin
- Maisonneuve, Gabriel
- Marchand, Antoine
- Mimeault, Justin
- Moeschler, Basile
- Renaud, Iris
- Scordino-Simondi, Jordan
- Troughton, Ailish
- Volle, Benjamin
- Wyper, Iona

4.2 Sponsors

Special thanks to:

AÉETS, Air Canada Cargo, Altair, Arkema, Bureau de fabrication ETS, CDCQ, Chem Trend, Composites One, CSL, Entrepôt Marine, ETS, FDDAEETS, Freeman Supply, Gurit, Hawkeye Ind., JLS Distribution, LAMSI, Loctite, Métaux Solution, Modèlerie GLT, Nautisme Québec, Novafor Equipement, PCM Innovation, Québec Yachting, Quincaillerie Notre Dame, Scott Bader, Siemens, Texonic, Voilerie Sansoucy, Yacht-Club Royal Saint-Laurent.

5 MARINESHIFT 360 LCA

5.1 General description

The purpose of this part is to conduct a theoretical analysis of the life cycle of the boat. This study was carried out using the MarineShift 360 tool, which specializes in Life Cycle Assessments (LCA) of boats. The actual analysis will be performed in the S2 report.

5.1.1 Functional unit

The functional unit serves as a common reference basis for measuring, comparing, and assessing the environmental impacts of product systems in an LCA. For the competition, the functional unit is as follows :

“The cradle-to-grave impacts of the entered vessel completing the 2024 Foiling SuMoth Challenge."

5.1.2 Outline

The MS360 webinar on March 1st, held by Tim Mollenhauer, presented the objective and boundaries of the analysis.

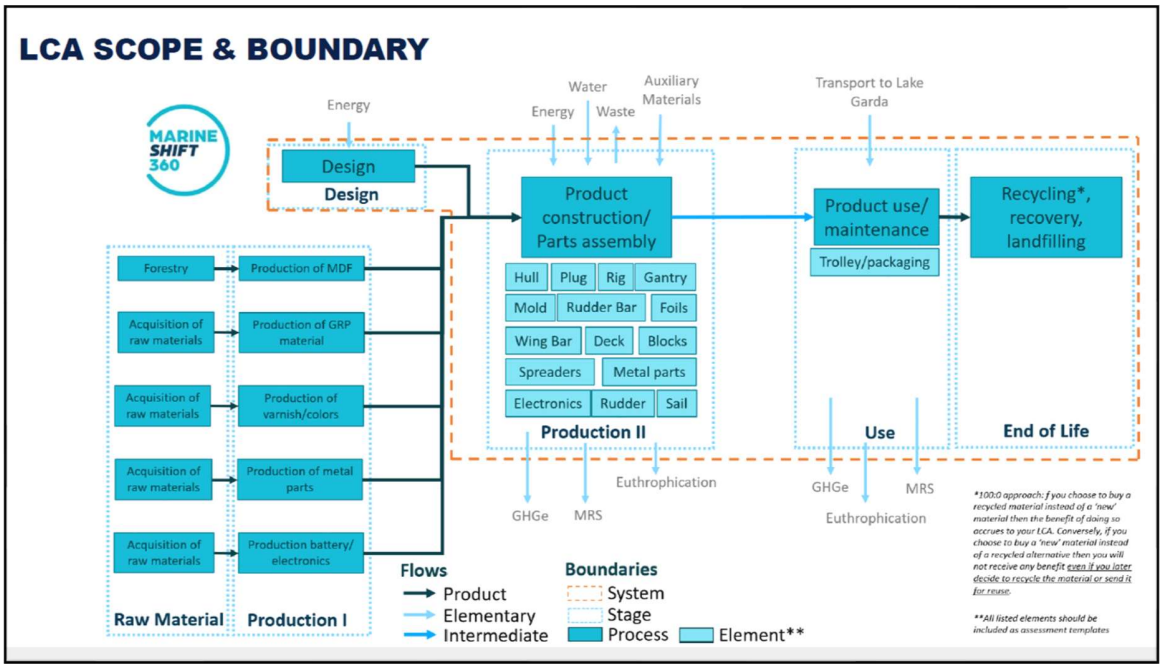

Figure 5.1 Scope and Boundaries of the LCA on MS360

5.1.3 Assumptions

For simplification, this theoretical LCA does not consider the packaging and transportation of materials. This work will be carried out in S2.

The mass of screws and bolts is less than 1% of the total mass of Rafale 3. Moreover, screws and bolts are made of recyclable materials: steel and aluminum. Thus, their impact is not included

in the analysis.

Most elements of the boat are recyclable at the end of life. Therefore, a recycling method (100:0) will be adopted where the benefit will not be attributed to the current team but to the future.

5.2 Boat and elements lifecycle

This part develops the modeling on MarineShift for each element of the boat. The expert template was used for most elements because it allows for much more precise detailing. The processes are grouped into a category to better analyze their impact in manufacturing. The quantities are the same as those estimated in the cost analysis table.

5.2.1 Hull

Table 5.1 Hull modeling on MS360

Item	Quantity (kg)	End of life
Plastic – PET (granulate/recycled)	500	Average recycling (100:0)
Plastic Resin - PMMA	30	Average recycling (100:0)
Dry fibers – Flax fibers (Global) (CO2 sequestration)	6	Average recycling (100:0)
Dry fibers – Carbon Standard Modulus	3	Average – Landfill municipal waste
Core – PET Foam (recycled)	5	Average – Landfill municipal waste

The mold is included in the modeling.

5.2.2 Gantry

Table 5.2 Gantry modeling on MS360

Item	Quantity (kg)	End of life
Plastic – PET (granulate/recycled)	35	Average recycling (100:0)
Plastic Resin - PMMA	1	Average recycling (100:0)
Dry fibers – Flax fibers (Global) (CO2 sequestration)	1	Average recycling (100:0)
Dry fibers – Carbon Standard Modulus	0.5	Average – Landfill municipal waste
Core – PET Foam (recycled)	0.3	Average – Landfill municipal waste

The mold is included in the modeling.

5.2.3 Hydrofoils

Table 5.3 Hydrofoils modeling on MS360

Item	Quantity (kg)	End of life
Timber - MDF	50	Average – Landfill municipal waste
Metal – Aluminium general (0% recycled)	4	Average – Landfill municipal waste
Plastic Resin - PMMA	5	Average recycling (100:0)
Dry fibers – Carbon Standard Modulus	3	Average – Landfill municipal waste
Dry fibers – Basalt fibre	2	Average recycling (100:0)
Resin – Epoxy / Petrolbased	0.6	Average – Landfill municipal waste

The mold is included in the modeling.

5.2.4 Wings

Table 5.4 Wings modeling on MS360

Item	Quantity (kg)	End of life
Plastic Resin – PET Resin – modelled as Granulate	2	Average – Landfill municipal waste
Plastic Resin - PMMA	3	Average recycling (100:0)
Dry fibers – Carbon Standard Modulus	1	Average – Landfill municipal waste
Dry fibers – Basalt fibre	1	Average recycling (100:0)
Dry fibers – Flax fibers (Global) (CO2 sequestration)	0.5	Average recycling (100:0)
Resin – Polyester Resin	0.1	Average – Landfill municipal waste

5.2.5 Wand

Table 5.5 Wand modeling on MS360

Item	Quantity (kg)	End of life
Plastic Resin – PET Resin – modelled as Granulate	0.05	Average – Landfill municipal waste
Plastic Resin - PMMA	0.3	Average recycling (100:0)

Item	Quantity (kg)	End of life
Dry fibers – Basalt fibre	0.01	Average recycling (100:0)

5.2.6 Rigging

Vang lever

Table 5.6 Vand modeling on MS360

Item	Quantity (kg)	End of life
Plastic Resin – PET Resin – modelled as Granulate	0.1	Average – Landfill municipal waste
Dry fibers – Carbon Standard Modulus	0.2	Average – Landfill municipal waste
Resin – Epoxy / Petrolbased	0.1	Average – Landfill municipal waste

Spreader

Table 5.7 Spreader modeling on MS360

Item	Quantity (kg)	End of life
Plastic Resin – PET Resin – modelled as Granulate	0.1	Average – Landfill municipal waste
Plastic Resin - PMMA	1	Average recycling (100:0)
Dry fibers – Carbon Standard Modulus	0.1	Average – Landfill municipal waste
Dry fibers – Flax fibers (Global) (CO2 sequestration)	0.3	Average recycling (100:0)
Resin – Polyester Resin	0.1	Average – Landfill municipal waste

Mast step

Table 5.8 Mat step modeling on MS360

Item	Quantity (kg)	End of life
Metal - steel Stainless	0.2	Average – Landfill municipal waste

Table 5.9 Fittings modeling on MS360

Item	Quantity (kg)	End of life
Casting Fitting – Stainless steel	1	Average – Landfill municipal waste
Casting Fitting – Aluminium (0% recycled)	0.4	Average recycling (100:0)
Material - Reused	1	Average – Landfill municipal waste
Rope - Nylon	0.15	Average – Landfill municipal waste

5.2.7 Consumables

Table 5.10 Consumables modeling on MS360

Item	Quantity (kg)	End of life
Consumable – Paint brush	20	Average – Landfill municipal waste
Consumable – Vacuum - Peelply	2	Average – Landfill municipal waste
Consumable – Vacuum – Vac sealant tape	8	Average – Landfill municipal waste
Consumable – Vacuum – High temp vac bag	5	Average – Landfill municipal waste
Consumable – Vacuum – Polyester breather	2	Average – Landfill municipal waste

5.2.8 Hardware

Table 5.11 Hardware modeling on MS360

Item	Quantity (kg)	End of life
Casting Fitting – Stainless Steel	0.5	Average – Landfill municipal waste
Electrical – Electronic for control unit (kg)	0.1	Average – Landfill municipal waste
Material - Reused	0.5	Average – Landfill municipal waste
Electrical – Electrical cabling	0.1	Average – Landfill municipal waste

5.2.9 Processes

The processes are modeled according to their electricity consumption. 3D printing, machining, oven use, vacuum pump use for infusions, and PC design phase are included in this category. An estimation of total electricity consumption was made:

Table 5.12 Processes modeling on MS360

Electricity	Quantity (kWh)
Electricity – Renewable – Hydro (electricity production high voltage)	1639

5.2.10 Transport of the boat

Only the transport of the boat is included in this modeling. The impact of passenger transport is discussed in part 5.

Table 5.13 Transport of the boat modeling on MS360

Air transport	Weight (kg)	Distance (km)
Transport – Air – Freight, aircraft, long haul flight	0.05	6136
Travel – Passenger – Road car	0.05	150

5.3 Results and analysis

Once all the data are entered on MS360, we can observe the results in the "Breakdown" tab. We will be able to look at the elements that have the most weight in the impact categories and compare them to the results of Rafale III.

5.3.1 Impact categories

For the impact category on fossil-based climate change, we obtain a carbon footprint of 1.92tCo2e. This value is roughly equivalent to a round trip between countries and Montreal by plane.

The hull is the part of the boat that emits the most, contributing one-third of the footprint. This is largely due to the use of recycled PET for the mold and Elium resin for the composite. Even though the PET from the mold is recycled, the use of 500kg is significant in the carbon balance. For Elium resin, it is recyclable, but the benefits will be seen in the future. Electricity production is the second most impactful part with an imprint of 441kgCO2e. This value is nevertheless overestimated because the electricity supplier Hydro-Québec announces an emission factor of 34g CO2e/kWh, which then gives, for a consumption of 10,000 kWh, an imprint of 340kg. In third place, the foils weigh the most with a contribution of 339kgCO2e mainly due to the use of carbon fiber.

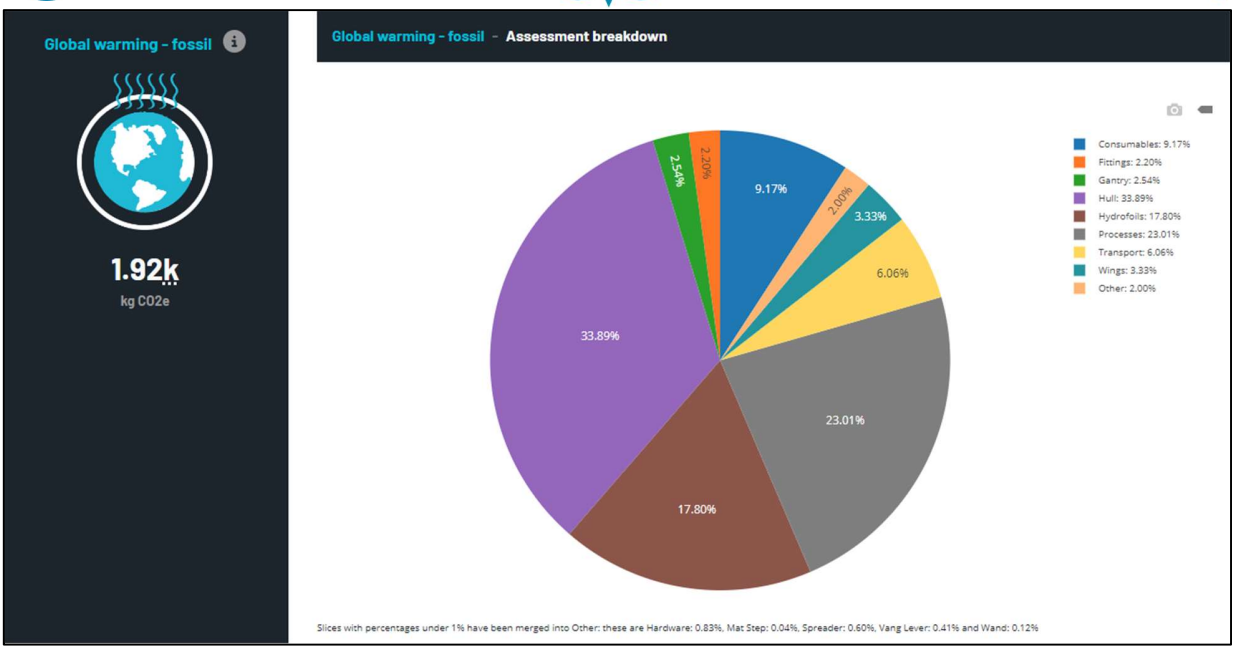

Figure 5.2 Rafale IV's impact on global warming (fossil)

In comparison, GHG emissions related to non-fossil energies are quite low with a value of 120kgCO2e. Again, the use of recycled PET for the hull mold is predominant.

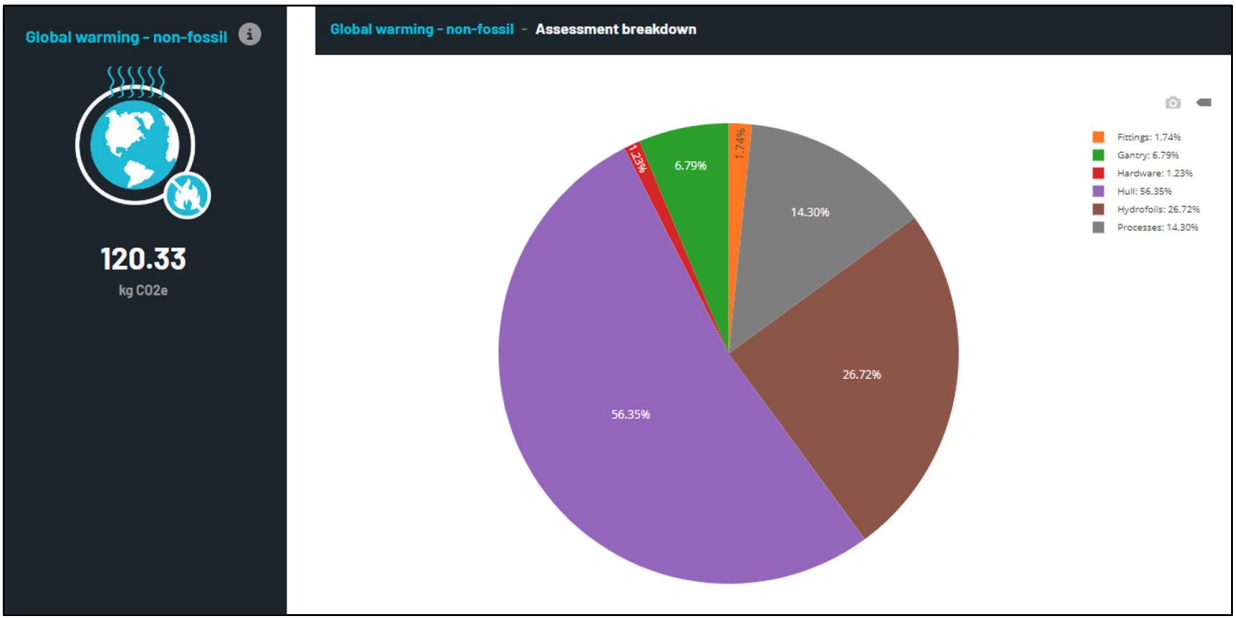

Figure 5.3 Rafale IV's impact on global warming (non fossil)

The impact on material availability is 3.69 kgCUe partly due to the aluminum used in the hydrofoils and the recycled PET from the hull mold.

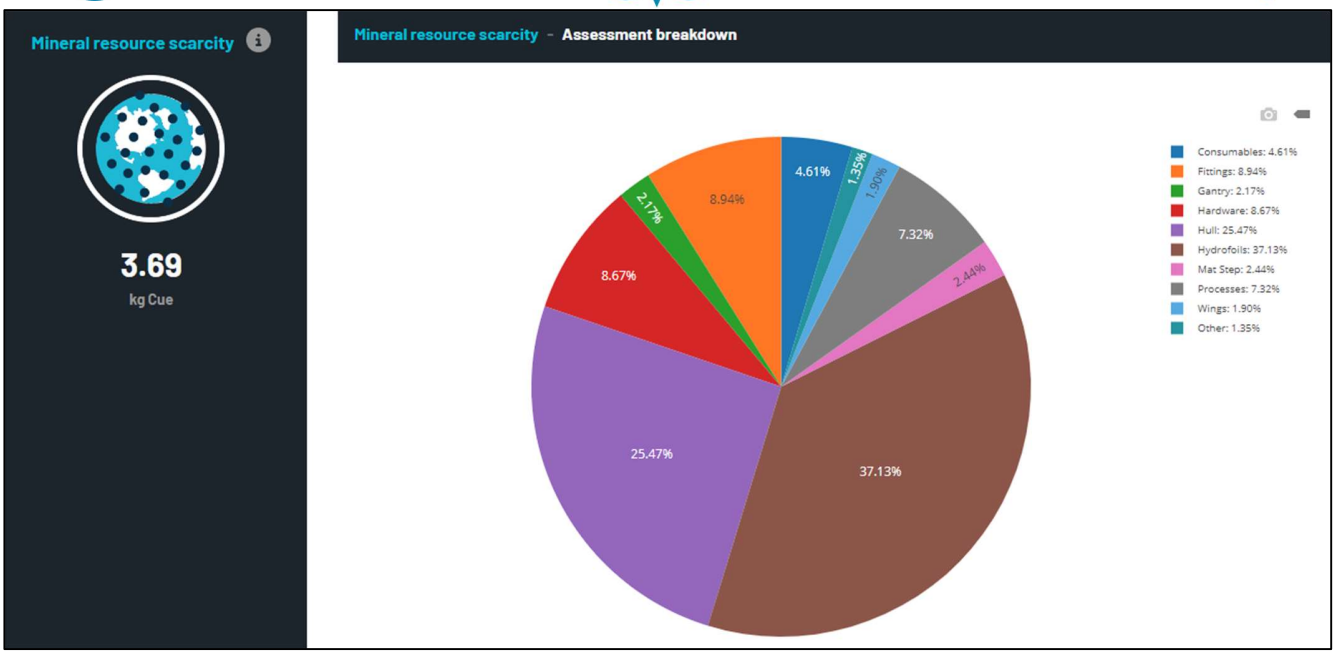

Figure 5.4 Rafale IV's impact on mineral resource scarcity

The non-renewable energy consumed is 31GJ with a large contribution from carbon fibers which require a lot of energy to be manufactured, as well as the recycled PET from the hull mold. It is surprising to find the processes with a contribution of 20% when they consume only hydroelectric energy. It would be interesting to see the calculation behind this with the Ecoinvent data used by MarineShift 360.

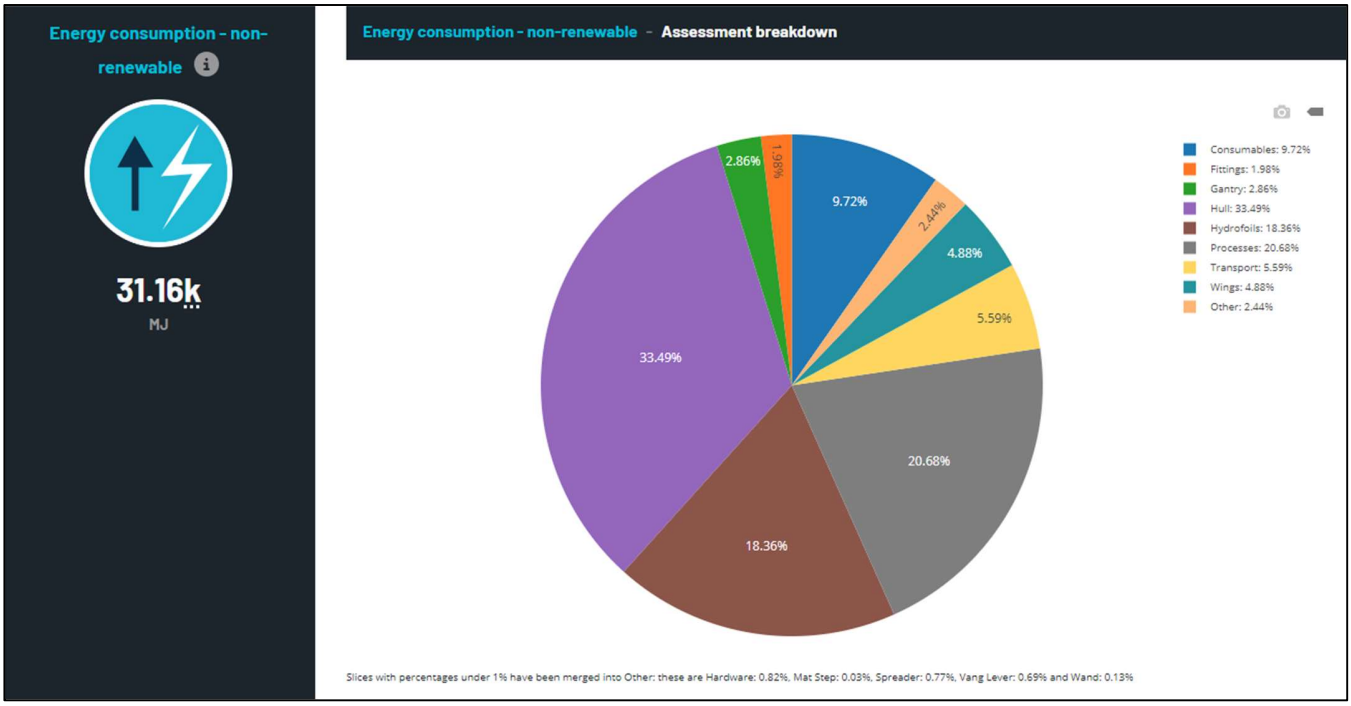

Figure 5.5 Rafale IV's impact on energy consumption (non-renewable)

Renewable energy consumption is 67% due to the processes that use hydraulic electricity from the Quebec mix.

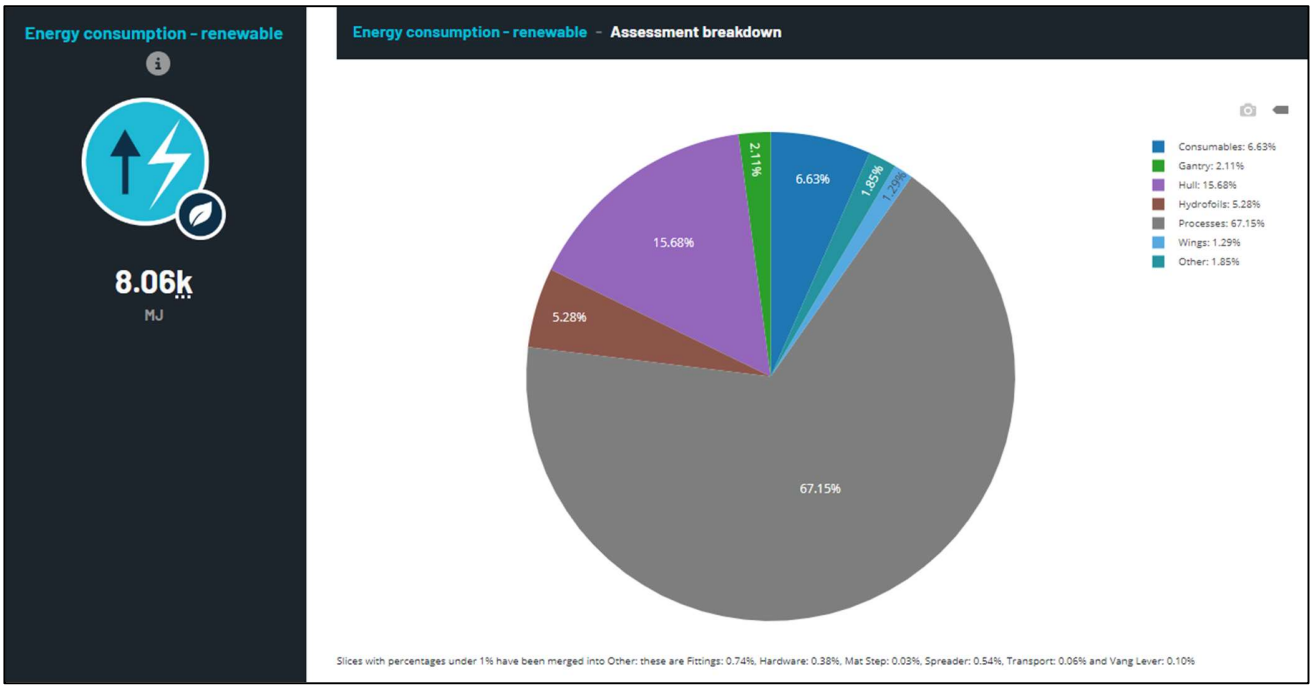

Figure 5.6 Rafale IV's impact on energy consumption (renewable)

Water consumption is 36m3 with 61% due to electricity consumption since it is of hydraulic origin. There is also a 20% contribution from the hull because flax requires a lot of water to grow.

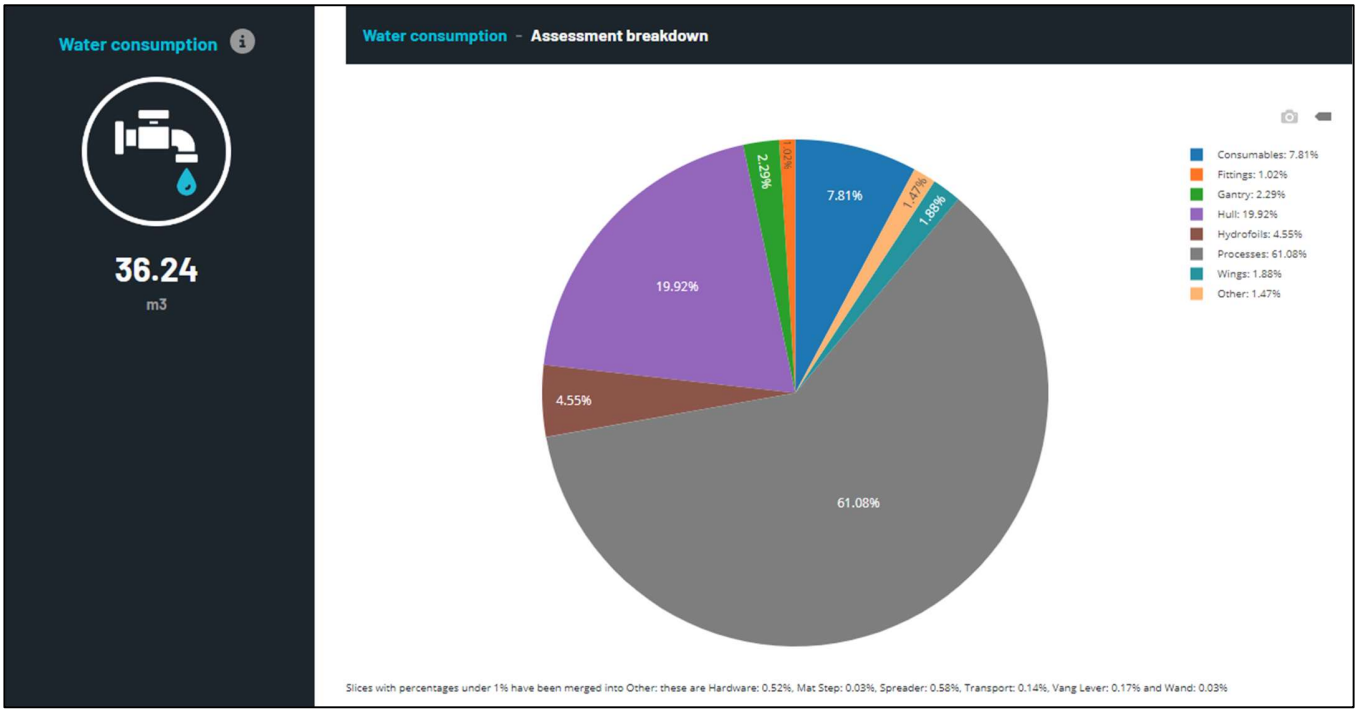

Figure 5.7 Rafale IV's impact on water consumption

Marine eutrophication is 0.34 kgNe once again dominated by the manufacture of the hull and the use of recycled PET.

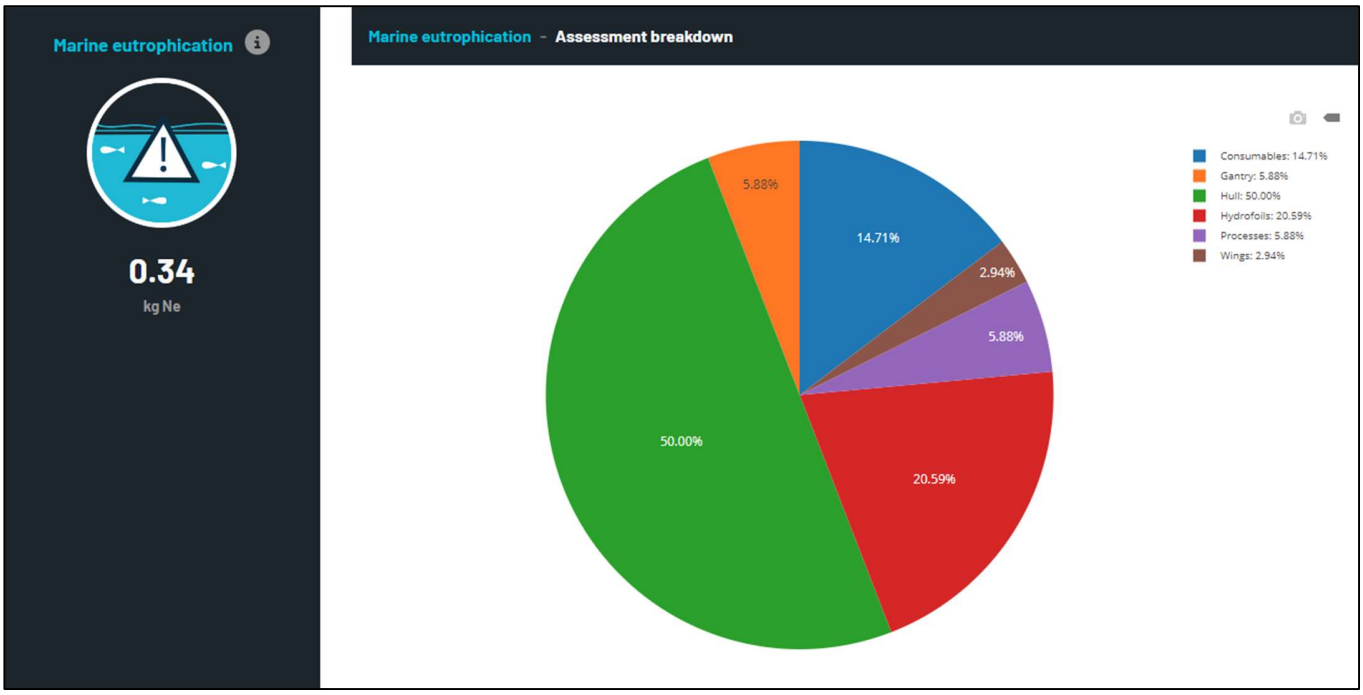

Figure 5.8 Rafale IV's impact on marine eutrophication

5.3.2 Team transportation

The Rafale team is the only one coming from another continent, which allows us to see the impact this has by possibly including the transport of the entire team in the life cycle analysis of the boat.

Table 5.14 Team transport modeling on MS360

Travel	Passengers (p)	Distance (km)
Travel – Passenger – Road car	12	150
Travel – Passenger – Air long haul flight	12	6136

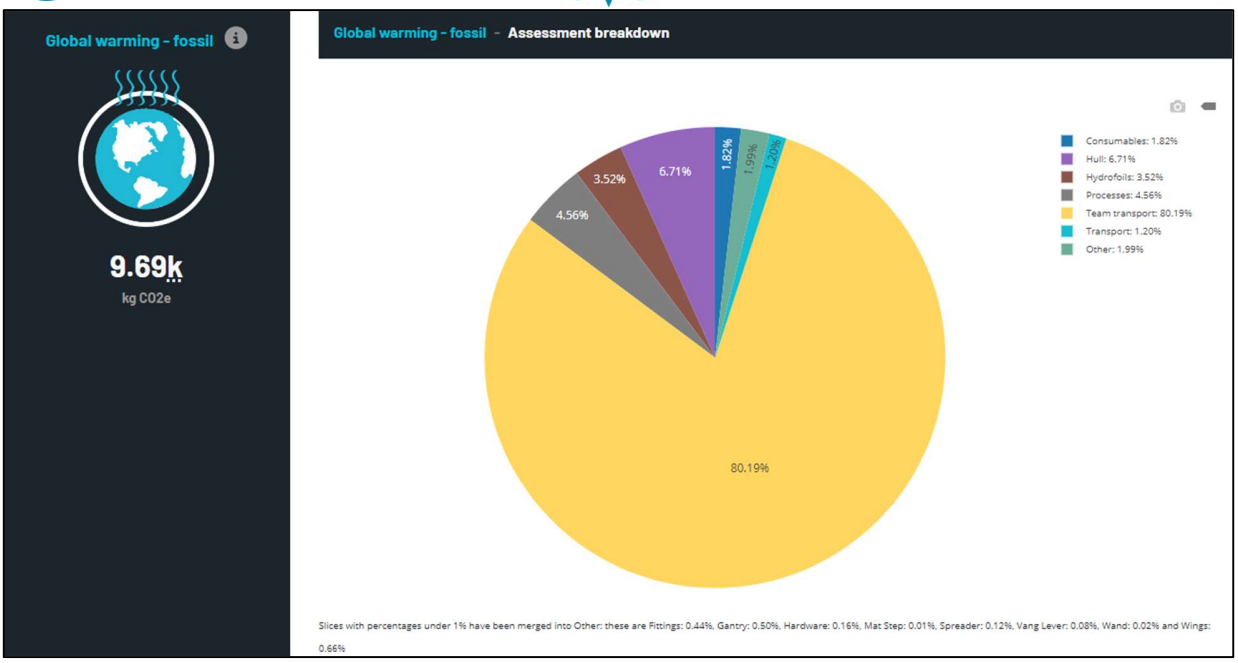

Figure 5.9 Impact of team transportation on the climate change category

The air travel of the team adds 7tCO2e to the carbon footprint of the boat and accounts for 80% of the climate impact. This confirms that Rafale is greatly disadvantaged by its North American origin. We have chosen to remove it from our analysis because this footprint masks the other elements of the boat that are interesting to analyze. However, even with this choice, the impact of team transport must be considered as it is a very important component of the analysis given its considerable impact on certain categories.

Including transportation has a similar effect on material availability and renewable energy consumption.

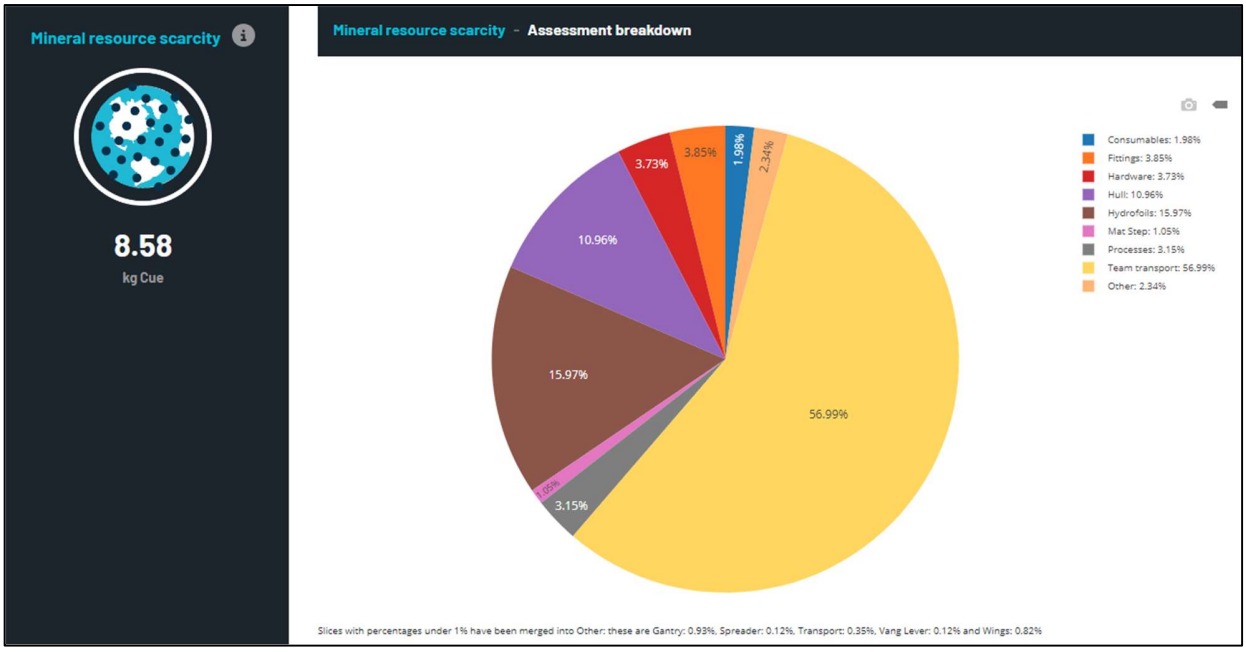

Figure 5.10 Impact of team transportation on the mineral resource scarcity category

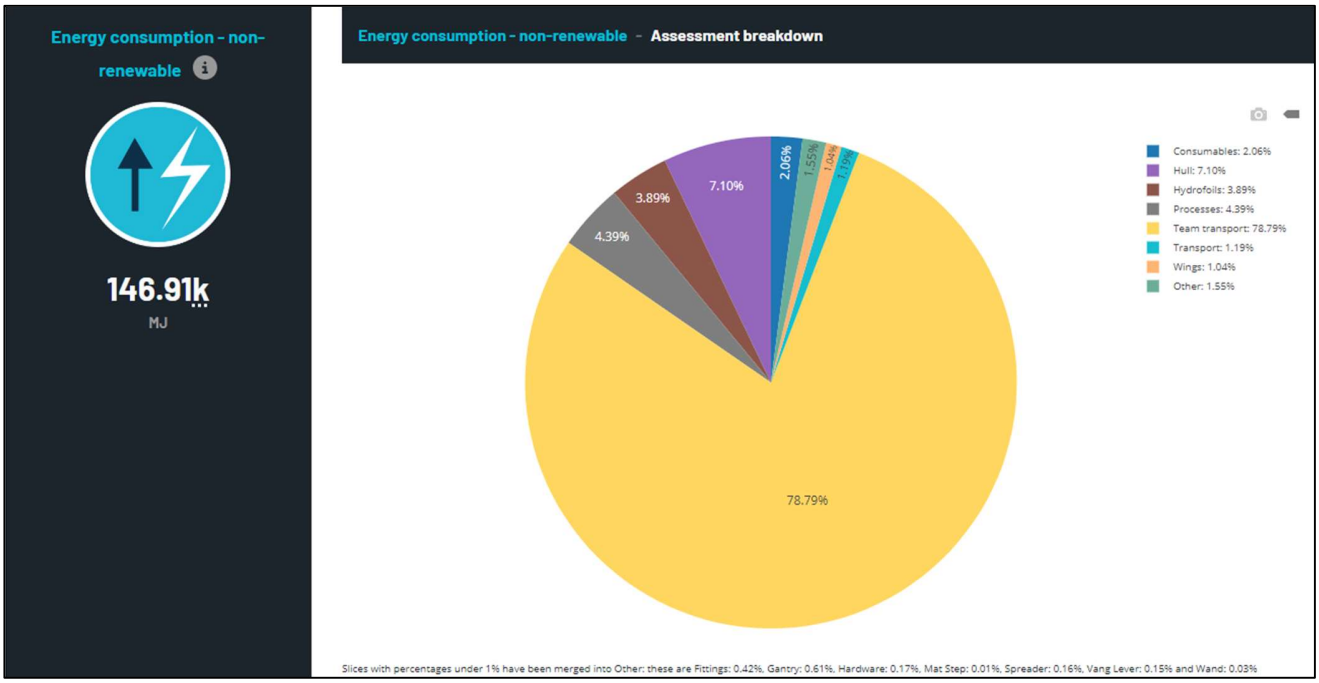

Figure 5.11 Impact of team transportation on the energy consumption (non-renewable) category

For other impact categories, the transport of the team has a lesser impact with contributions ranging from 5 to 8%.

5.3.3 Rafale III & IV comparison

It is also interesting to compare Rafale III and IV to see if the new sustainable approach we have imagined is more effective than the old one. For example, we can look at the impact of the two boats on climate change.

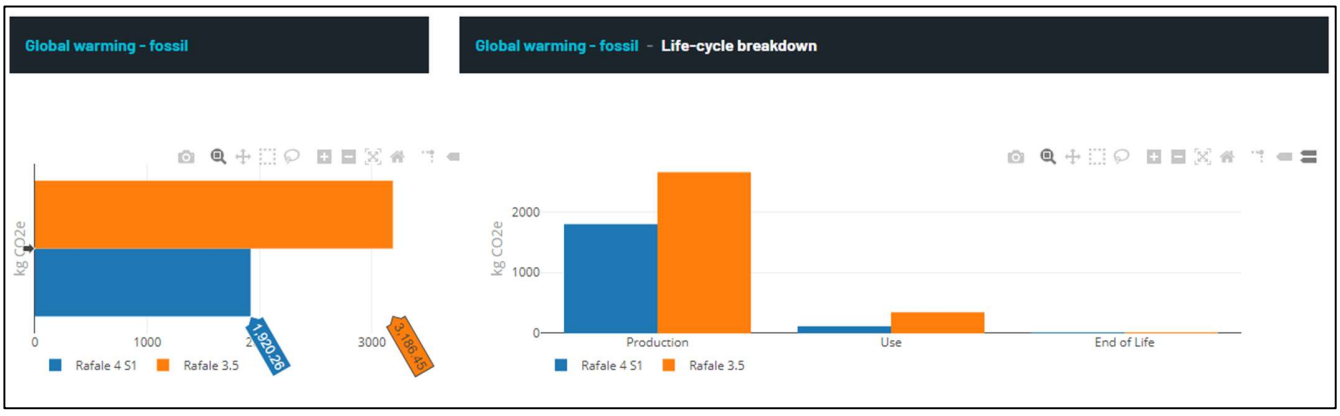

Figure 5.12 Comparison of the impact of Rafale IV and III on climate change (fossil)

Theoretically, Rafale IV emits 1.3tco2e less than Rafale III, which is a great success in our approach to reducing GHG emissions during production.

We can also compare for non-fossil origin climate changes.

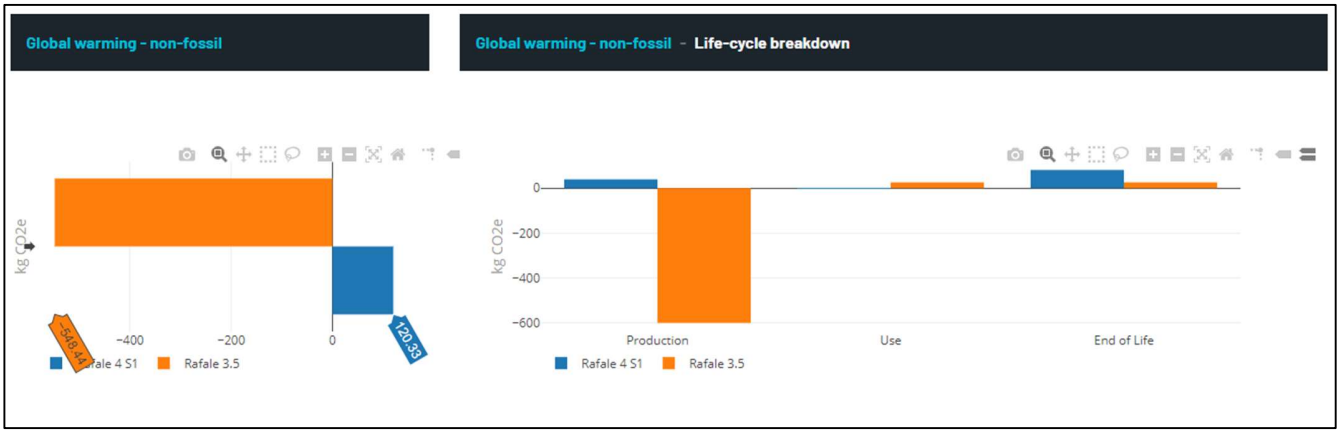

Figure 5.13 Comparison of the impact of Rafale IV and III on climate change (non fossil)

In this case, Rafale III is better because the hull of the boat had been made of wood (pine), which is a material that captures a large amount of CO2 during its life cycle. However, considering both fossil and non-fossil emissions, Rafale IV emits less.

Otherwise, Rafale IV has a lower impact in all other categories such as resource consumption and marine eutrophication. The same goes for categories not represented below.

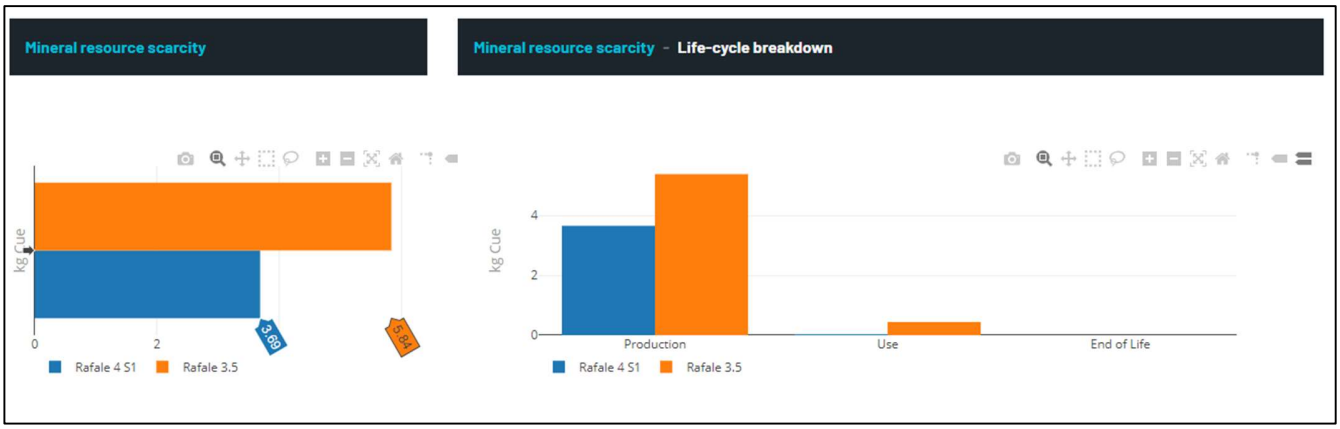

Figure 5.14 Comparison of the impact of Rafale IV and III on mineral resource scarcity

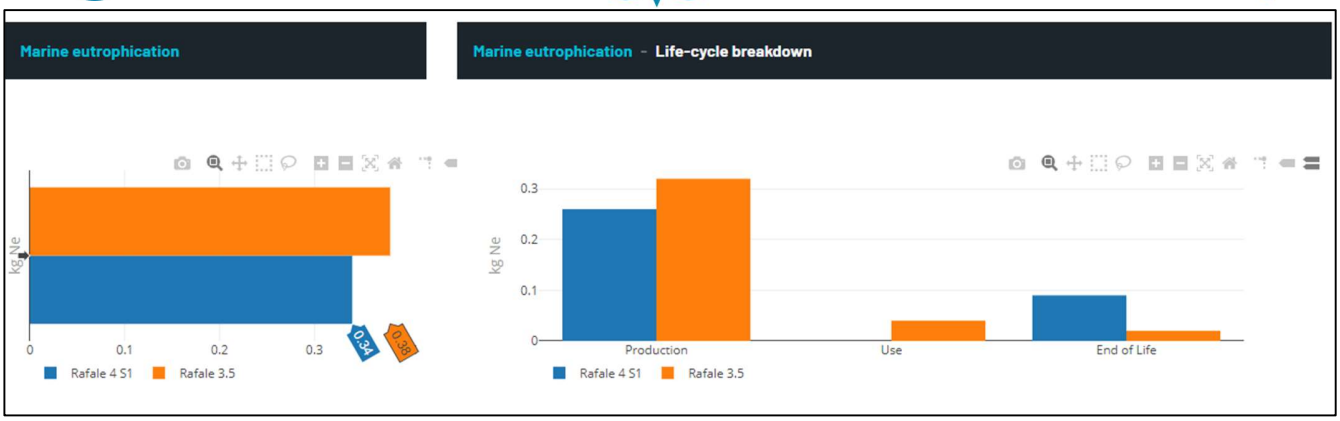

Figure 5.15 Comparison of the impact of Rafale IV and III on marine eutrophication

5.4 Conclusion

In theory, Rafale IV is more environmentally friendly than its predecessor. The decisions that have been made allow for a significant reduction in GHG emissions and impacts on other categories. The hull, specifically its mold, is undoubtedly the part of the boat with the largest contribution as it is made of recycled PET. The wooden mold of Rafale III had the particularity of being more environmentally friendly but could not be reused because the wood cracks after a few months due to humidity. Recycled and recyclable PET was therefore used to make the mold for the new hull. It will be reused for future versions of Rafale, and we could have amortized the mold over the number of hull productions to be more precise. The estimates from this analysis are encouraging and show that our team is improving year by year by increasingly adopting a life cycle approach. The S2 report will be an opportunity to confirm or not this analysis and see the differences between theory and reality once the boat's construction is completed.

6 BIBLIOGRAPHY

R.Ponter, L. Sutherland & Y. Garbatov. 2022 « Structural analysis of a 'Foiling Moth' sailing dinghy hydrofoil ».

Ashby, M. F. (2011). *Materials selection in mechanical design* (4th ed.). Burlington, MA : Butterworth-Heinemann. Repéré à http://www.dawsonera.com/depp/reader/protected/external/AbstractView/S9780080952239

Ashby, Michael F., & Dupeux, M. (2011). *Matériaux et environnement : choix éco-responsable en conception*. Paris : L'Usine nouvelle. Repéré à http://catalogue.bnf.fr/ark:/12148/cb425240736

Hollaway, L. (Leonard). (1994). *Handbook of polymer composites for engineers*. Cambridge : Woodhead Publishing Ltd. Repéré à http://public.ebookcentral.proquest.com/choice/publicfullrecord.aspx?p=1640096

Soden, P. D., Kaddour, A. S., & Hinton, M. J. (2004). Recommendations for designers and researchers resulting from the world-wide failure exercise. *Composites Science and Technology*, *64*(3-4), 589-604. https://doi.org/10.1016/S0266-3538(03)00228-8

A. APPENDIX A

A.1. Technical requirements

Code	Name	Criteria	Levels	Acceptability class	Acceptability limit
FS - 1	Flying when sailing	Flying duration	> 15 min	F1	> 5 min
FS - 2	Sailing in floating mode	Yes / No	Yes	F0	/
FS - 3	Being able to change direction on water	Yes / No	Yes	F0	/
FC - 2	Being unsinkable	Stay on the surface in all circumstances with a skipper of:	85kg	F0	/
FC - 3	Being wind powered	Wind speed	8 - 16 kn	F1	9 - 15 kn
FC - 9	Respect the *International Moth* rules	Yes / No	Yes	F0	/
FC - 10	Being transportable by plane/boat/big car	Yes / No	Yes	F0	/
FC - 12	Having a minimal equivalent carbon impact	Total CO2eq emissions	< 2000 kg	F1	< 2300 kg
FC - 13	Being repairable	Damages type	Small	F2	Tiny
FC - 1	Taking-off early	Takeoff speed	5kn	F1	7kn
FC - 5	Being light	Mass	< 45 kg	F2	< 55 kg
FC - 17	Having an adjustable flight height	Adjustment range	50 cm	F2	30 cm
FC - 18	Having an adjustable sensitivity	Yes / No	Yes	F0	/
FC - 19	Having an aable pitch	Angle range of rudder foil	+/- 7°	F0	+/- 5°
FC - 20	Allowing sail shape adjustments	Yes / No	Yes	F0	/
FC - 7	Being relatively simple to sail	Level of skipper	Medium	F1	High
FC - 21	Sailing fast on the foils	Max speed	>25kn	F2	>17kn
FC - 8	Being able to sail with small waves	Wave height	< 50 cm	F2	< 25 cm
FC - 11	Being quick to rig	Time to rig (2 people)	20 min	F3	45 min
FC - 15	Resisting to the sun heat	Max surface temperature	80°C	F2	50°C
FC - 16	Résisting to UV rays	Time to UV weathering	10 years	F3	3 years
FC - 4	Measuring navigation data	Yes / No	Oui	F3	Non
FC - 14	Being aesthetic	% of satisfied people	80%	F3	20%

A.2. FEA for the hull

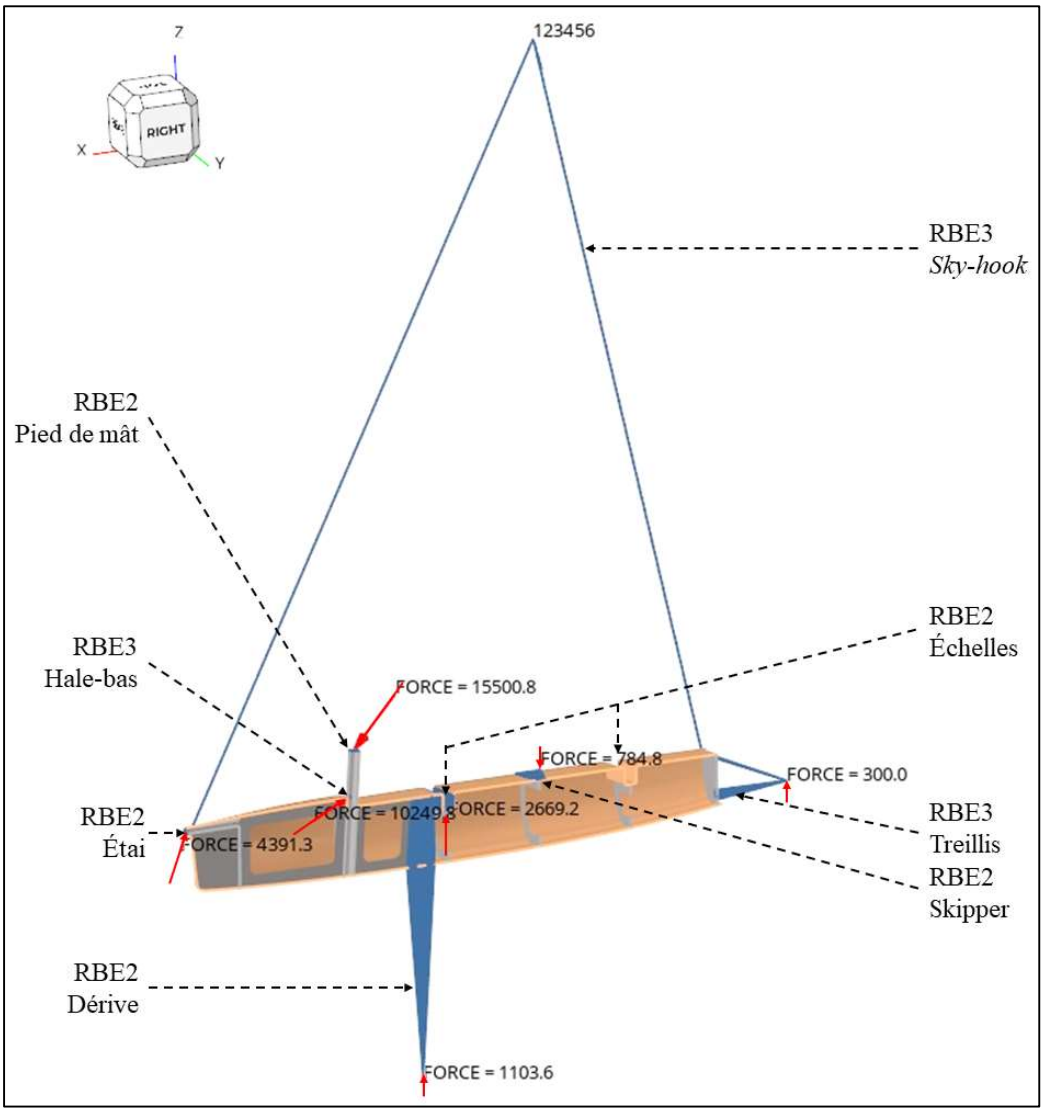

Sectional view of the finite element model of the hull subjected to load n°1

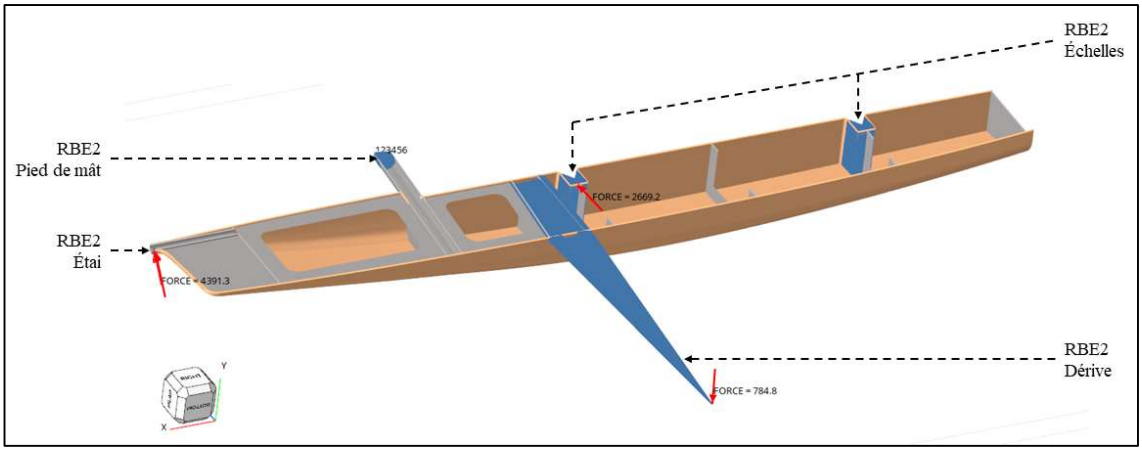

Sectional view of the finite element model of the hull subjected to load n°1

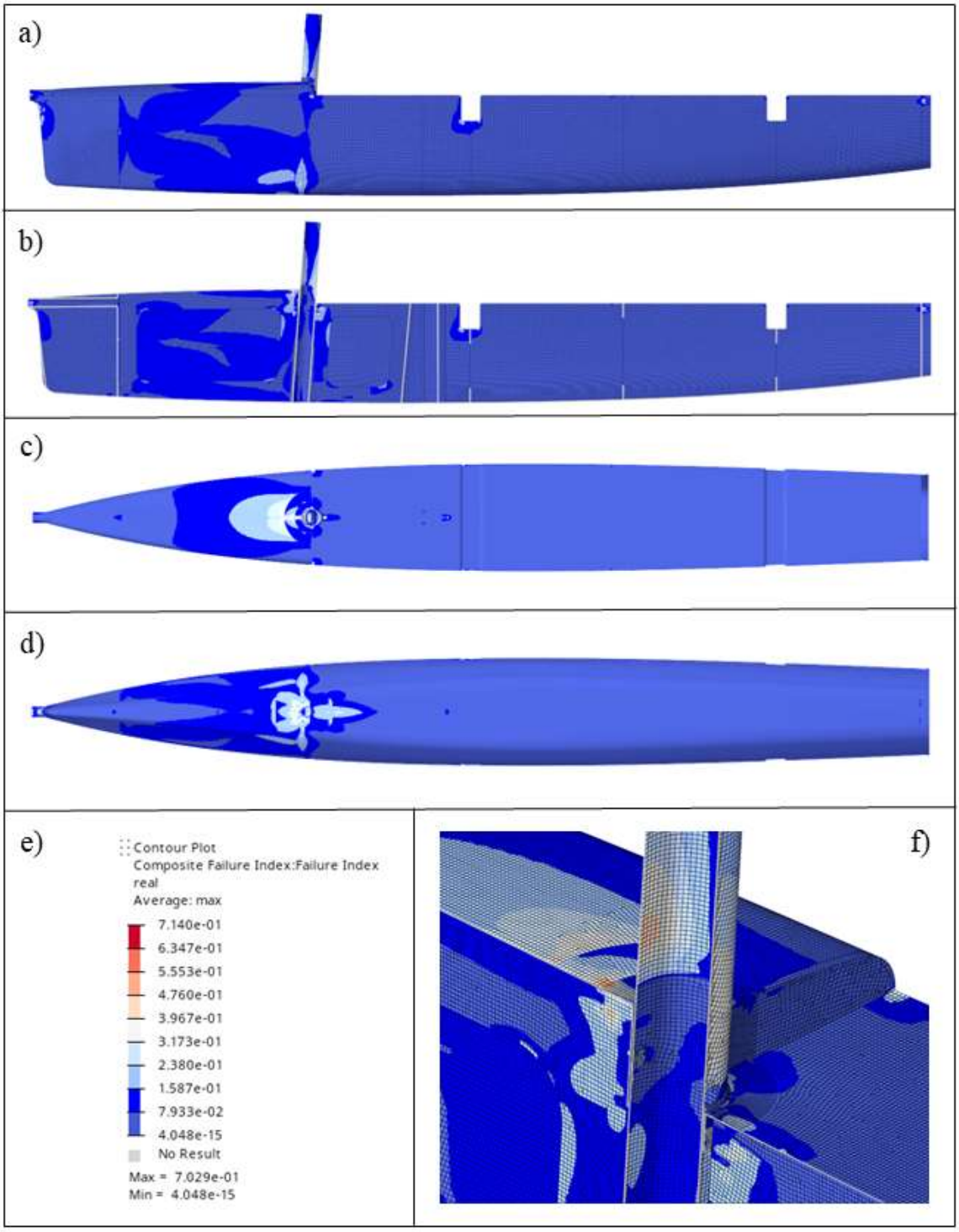

Failure index for load case 1: port view (a), port cross-section (b), top view (c), bottom view (d), detail view (f) and scale view (e)

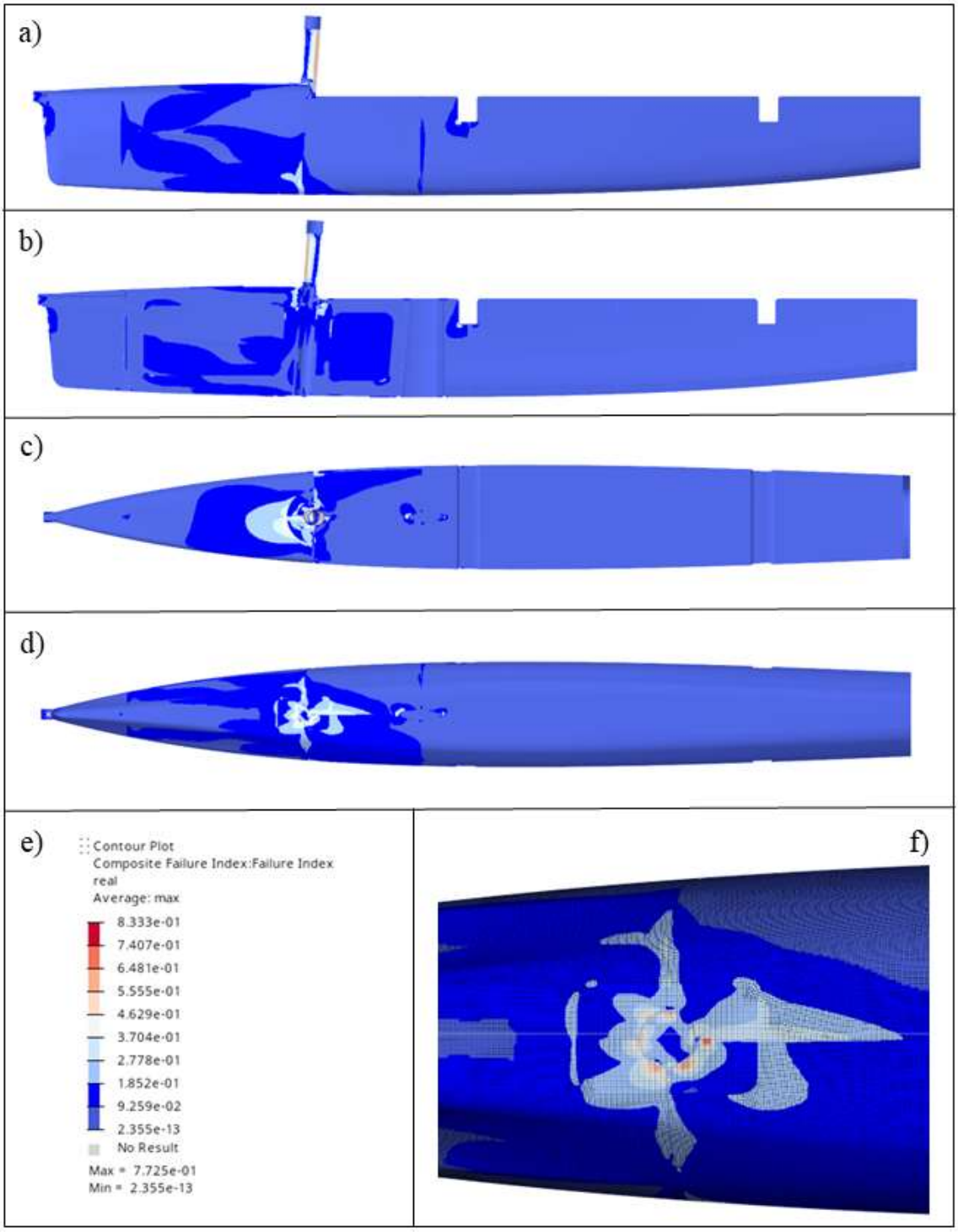

Failure index for load case 2: port view (a), port cross-section (b), top view (c), bottom view (d), detail view (f) and scale view (e)

A.3. Onboard system datasheets

GPS:

https://content.u-blox.com/sites/default/files/ZED-F9P-04B_DataSheet_UBX-21044850.pdf

Accelerometer/gyroscope:

https://www.ceva-ip.com/wp-content/uploads/2019/10/BNO080_085-Datasheet.pdf

Raspberry Pi 4 model B:

https://datasheets.raspberrypi.com/rpi4/raspberry-pi-4-datasheet.pdf

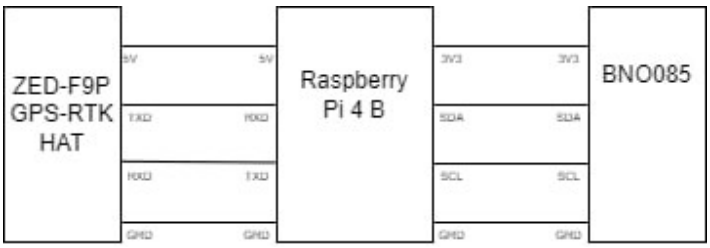

Raspberry Pi 4B schematic

A.4. FEM of the hydrofoil system

Structural analysis of the shaft

To simplify the analyses, the daggerboard is considered hollow. In practice, an internal core is glued into the daggerboard. This core slightly aids in shear recovery and reduces the buckling effect. The daggerboard is held in the boat's hull over a length of 0.4m. This ensures proper support of the daggerboard and allows it to be considered as fixed at this point (right figure).

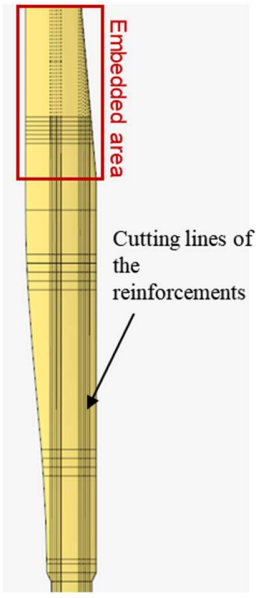

Shaft imported in Altair

The daggerboard is composed of the following laminate: firstly, two layers of woven carbon fiber are applied for protection. Then, six layers of basalt, applied with orientations of +-30 degrees, are applied. These layers help shape the daggerboard and absorb the shear applied to it. Finally, twelve reinforcements are used to absorb the flexion of the daggerboard along its entire length. They are all oriented at an angle of 0 degrees. The various reinforcements do not all have the same dimensions. On one hand, the stresses become more significant at the hull level (maximum moment of force). In this area, more reinforcements are added. Additionally, to avoid accumulations, the different reinforcements are cut with offsets relative to each other (adjacent figure). This prevents abrupt section changes. In total, there are 12 carbon reinforcements. The largest reinforcement measures (9x120) cm and the smallest measures (4x30) cm (figure below). This ply arrangement significantly reduces the carbon mass compared to the daggerboards of Rafale 3 and 3.5. Basalt accounts for approximately 45% of the composite

fiber mass. The material data for basalt are derived from an article published in the "Journal of Composites Science" [11]. Meanwhile, the carbon data are those commonly used by the Rafale club for simulations.

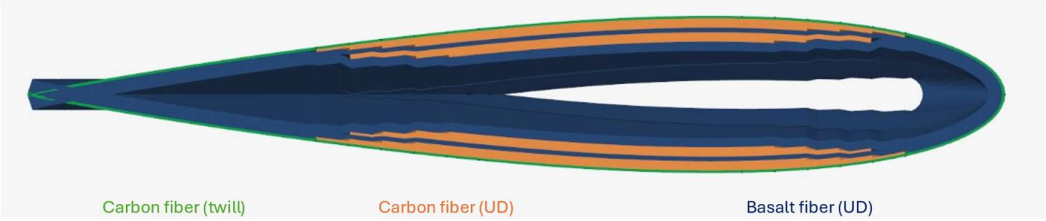

Ply of the daggerboard shaft

Loading cases for the daggerboard

Two loading cases are then applied. The first is a force applied to the tip of the daggerboard. This loading case aims to verify the rigidity of the daggerboard under a tip force of 500 newtons. The second case is an extreme pressure case that could potentially occur during an accident. This pressure is defined in the design requirements and corresponds to 0.035 megapascals distributed over the submerged part of the daggerboard.

Results of daggerboard stiffness

The daggerboard exhibits a maximum deflection of 30 millimeters when a force of 500 newtons is applied to the tip of the foil. This result confirms that the daggerboard will not move too much during standard flight. The deflection is zero at the attachment point and becomes increasingly significant at the bottom of the daggerboard. This demonstrates that the loads and fixation have been correctly applied to the model.

Results of daggerboard strength

To determine if the daggerboard is at risk of breaking during an accident, the maximum pressure case is utilized. The Hashin resolution technique is used for analysis. The results indicate a safety factor of 2.0 (Failure Index of 0.49). The minimum factor is found at the base of the daggerboard where the moment of force is highest. The failure mode is compression of the fibers, which will yield first (Figure below). Maintaining a good safety factor is important in case of manufacturing uncertainties. Additionally, the accident pressure is an estimated value, which could potentially be higher.

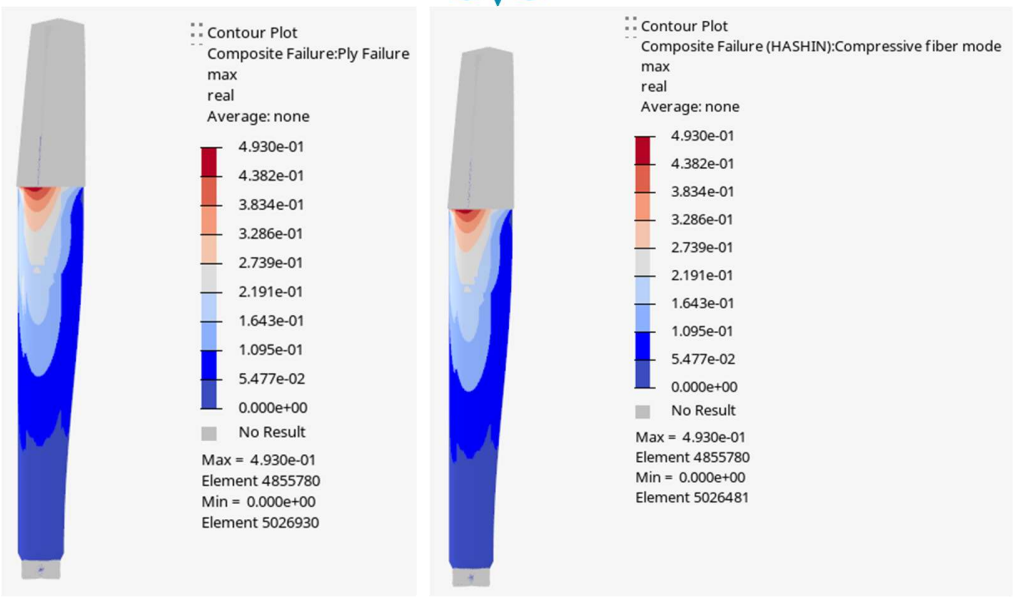

Results of daggerboard strength with composite failure index and compressive failure index

Structural analysis of the hydrofoil system

The daggerboard shaft is imported into the new analysis as presented in the previous section. The two aluminum junction pieces are added as solid bodies. The different elements are connected to each other using fixed contact. This case is an ideal scenario. However, it is possible to extract the stresses present on the different elements in contact. These stresses help validate if the adhesive surface is sufficient to hold the pieces together. The joining surfaces of the two metal pieces are linked together infinitely rigidly. The wing is then added as a surface (figure below). The flap is neglected in the analysis since it experiences little load, with most of the load being carried by the control bar. The part of the wing that bears the most load is located near the leading edge. In the center of the wing, a reinforced plastic (Nylon 6 - GF) core is inserted to prevent the metal piece from crushing the two carbon shells of the wing against each other. This piece is meshed with coarser 3D elements.

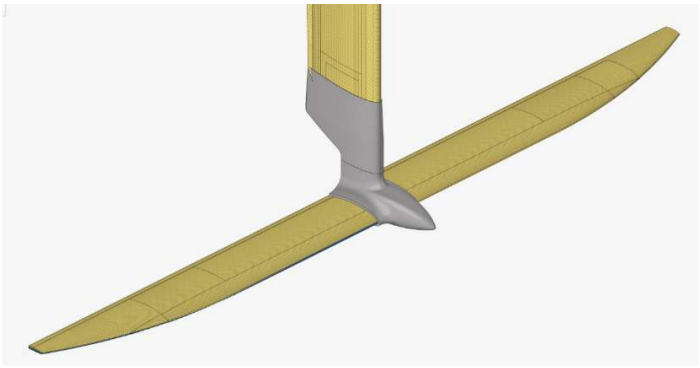

Mesh of the wing and the junction pieces

The wing is made of prepreg. All plies are carbon fiber. The first ply is woven carbon to withstand various impacts. Subsequent plies are unidirectional. The majority have a 0-degree angle in the

spanwise direction. Six plies are positioned with angles of +/-30 degrees to counteract residual torsion. Like the rudder, smaller reinforcements address the bending moment. In total, there are 20 plies of unidirectional carbon fiber.

Loading cases

The first loading case is flight pressure (figure below - top). This pressure corresponds to the flight force divided by the wing's surface area. This case verifies the maximum deflection of the wing during normal flight. The second case involves a force equal to the weight of the boat applied only on one side of the wing at one-quarter of the span. This force ensures that the wing and the junction do not fail if the sailboat generates too much lift. In this scenario, only half of the wing remains submerged. The loading values are defined by the requirements (figure below - bottom).

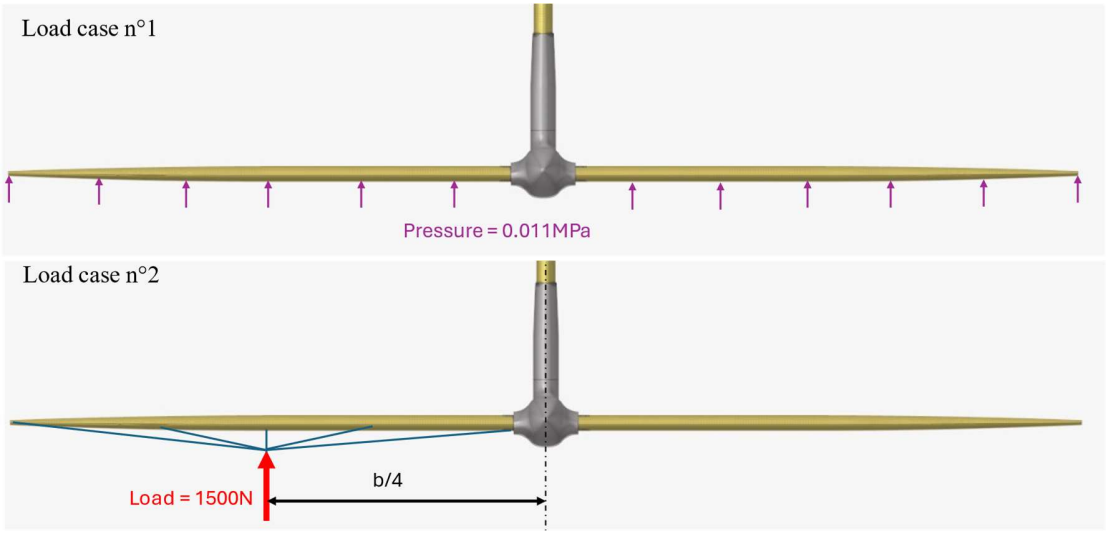

Presentation of the loading cases

Flight Deflection Results of the Wing

The results of the flight case show a maximum deformation of 8.9 millimeters at the wingtip (figure below). According to the requirements, this value should not exceed 10 millimeters to maintain proper operation of the flap. Therefore, the flap should remain functional during flight. As the pressure is symmetrically distributed relative to the rudder, it is only minimally deformed.

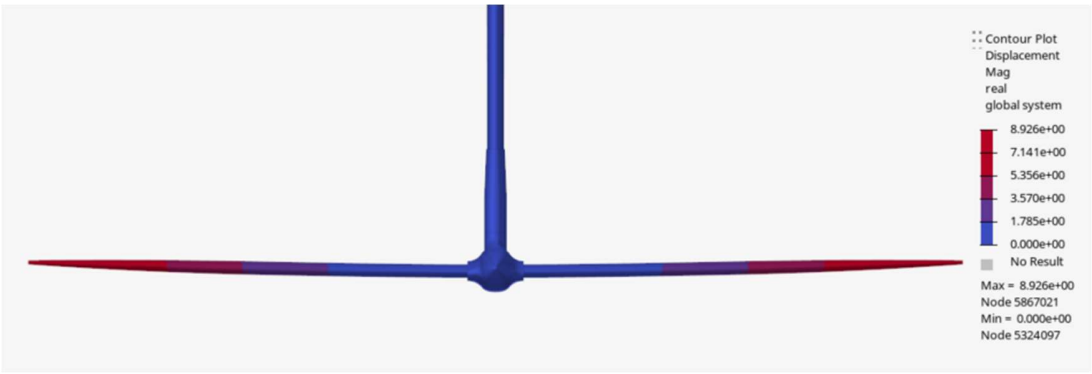

Deflection results

Results of Maximum Force in Case of Excessive Lift

This scenario aims to verify that both the wing and the metal parts are sufficiently resilient. The von Mises stresses within the metal parts are examined. The highest value is 377 megapascals. However, this value represents a residual stress located on an edge of the wing junction piece. By adjusting the maximum value on the stress plot, it is observed that the stress at the junction, which is at risk of breaking, is approximately 160 megapascals (Figure below). According to the aluminum datasheet, the yield strength is 255 megapascals, and the ultimate tensile strength is 315 megapascals. Therefore, the stress at the fracture location is below the yield strength (safety factor of 1.5).

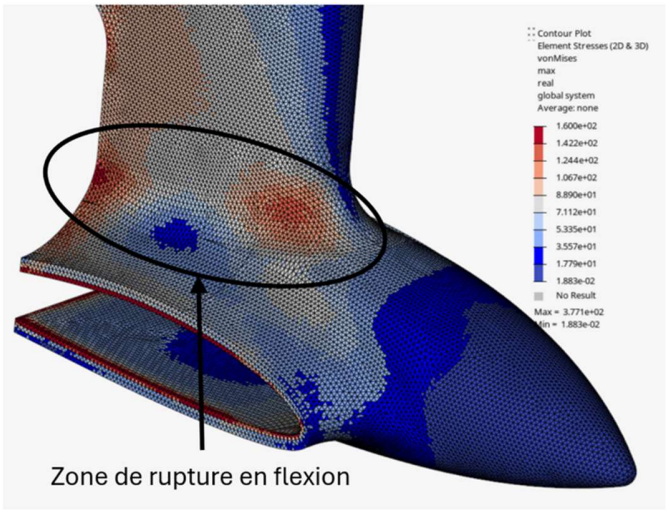

Results of von Mises stresses on the metal parts

For the wing, the results of the Ashin ply failure safety factor are observed. Firstly, the visualization of this factor shows a standard distribution of bending. A Composite Failure Index of 0.55 is present (safety factor of 1.8). The primary mode of failure is in the fiber under compression with a Failure Index of 0.47 (figure below). It's crucial to maintain a good safety factor. The prepreg used is expired, which may decrease the structural characteristics, especially for the resin.

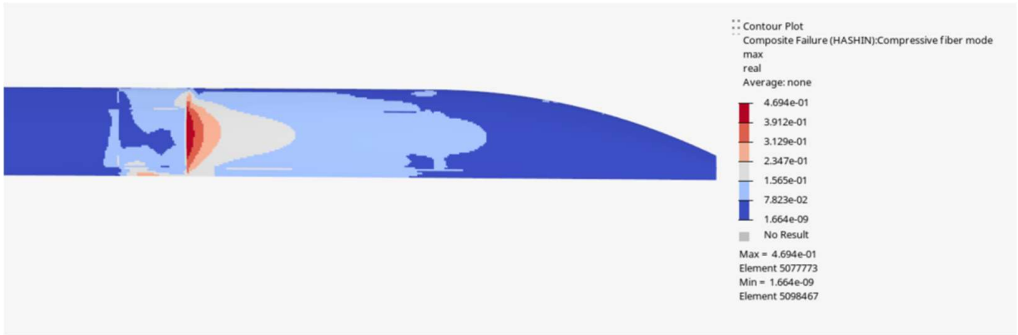

Results of composite ply failure on the wing